U-Pb Zircon geochronology of the Cambro-Ordovician metagranites and metavolcanic rocks of central and NW Iberia

Talavera, C.[1,2], Montero, P. [1], Bea, F. [1], González Lodeiro, F. [3], Whitehouse, M. [4]

[1] Department of Mineralogy and Petrology, Campus Fuentenueva, University of Granada, 18002 Granada, Spain. Ph: +34 958 248 535.Fax: +34 958 243 368. email:cristal@ugr.es

[2] Research School of Earth Sciences, Australian National University, Canberra, ACT, 0200, Australia.

[3] Department of Geodinamics, Campus Fuentenueva, University of Granada, 18002 Granada, Spain

[4] Swedish Museum of Natural History, Box 50007, SE-104 05 Stockholm, Sweden.

Abstract

New U-Pb zircon data from metagranites and metavolcanic rocks of the Schist-Graywacke Complex Domain and the Schistose Domain of Galicia Tras-os-Montes Zone from central and NW Iberia contribute to constrain the timing of the Cambro-Ordovician magmatism from Central Iberian and Galicia Tras-os-Montes Zones which occurred between 498 and 462 Ma. The crystallization ages of the metagranites and metavolcanic rocks from the Northern Schist-

Graywacke Complex Domain are: a) In west Salamanca, 489 ± 5 Ma for Vitigudino, 486 ± 6 Ma for Fermoselle and 471 ± 7 Ma for Ledesma; b) In northern Gredos, 498 ± 4 Ma for Castellanos, 492 ± 4 Ma for San Pelayo and 488 ± 3 Ma for Bercimuelle; c) In Guadarrama, 490 ± 5 Ma for La Estación I, 489 ± 9 Ma for La Cañada, 484 ± 6 Ma for Vegas de Matute (leucocratic), 483 ± 6 Ma for El Cardoso, 482 ± 8 Ma for La Morcuera, 481 ± 9 Ma for Buitrago de Lozoya, 478 ± 7 Ma for La Hoya, 476 ± 5 Ma for Vegas de Matute (melanocratic), 475 ± 5 Ma for Riaza, 473 ± 8 Ma for La Estación II and 462 ± 11 Ma for La Berzosa; and d) In Toledo, 489 ± 7 Ma for Mohares and 480 ± 8 Ma for Polán. The crystallization ages of the metagranites from the Schistose Domain of Galicia Tras-os-Montes Zone are 497 ± 6 Ma for Laxe, 486 ± 8 Ma for San Mamede, 482 ± 7 Ma for Bangueses, 481 ± 5 Ma for Noia, 480 ± 10 for Rial de Sabucedo, 476 ± 9 Ma for Vilanova, 475 ± 6 Ma for Pontevedra, 470 ± 6 Ma for Cherpa and 462 ± 8 Ma for Bande. This magmatism is characterized by an average isotopic composition of $(^{87}Sr/^{86}Sr)_{485Ma} \approx 0.712$, $(\varepsilon_{Nd})_{485Ma} \approx -4.1$ and $(T_{DM}) \approx 1.62$ Ga, and a high zircon inheritance, composed of Ediacaran-Early Cambrian (65%) and, to a lesser extent, Cryogenian, Tonian, Mesoproterozoic, Orosirian and Archean pre-magmatic cores. Combining our geochronological and isotopic data with others of similar rocks from the European Variscan Belt, it may be deduced that Cambro-Ordovician magmas from this belt were mainly generated by partial melting of Ediacaran-Early Cambrian igneous rocks.

Keywords: Cambro-Ordovician, magmatism, U-Pb dating, zircon

1. Introduction

The Pre-Variscan basement of the Iberian Massif, in general, and the Central Iberian Zone, in particular, contains numerous Lower Ordovician magmatic rocks (Fig. 1). The Central Iberian Zone is bounded to the north by the Cambro-Ordovician, mostly metavolcanic rocks, of de Ollo de Sapo Formation (470 Ma - 495 Ma (Bea et al. 2006; Montero et al. 2007; Montero et al. 2009; Díez Montes et al. 2010)) and to the south by the similar, but less voluminous, Urra Formation (488-495 (Sola et al. 2008)). Besides, inside the Central Iberian Zone there are two main areas of pre-Variscan magmatic rocks. One, known since old, located in the northern part of the Schist-Graywacke Complex Domain including the gneisses of Guadarrama, Salamanca, Zamora and Toledo (hereafter called the Castilian gneisses), strongly affected by the Variscan deformation and metamorphism. The other, recently discovered, is located in the southern part of the Schist-Graywacke Complex Domain; it includes de plutons of Gouveia (Neiva et al. 2009), Oledo (Antunes et al. 2009) and Zarza la Mayor (Corretgé et al. pers. com.) formed of unmetamorphosed and almost undeformed granites previously believed to be Variscan. The lineations of Castilian gneisses apparently continues towards the NW, in Schistose Domain of the Galicia Tras-os-Montes Zone (Fig. 1), where small bodies of metagranites (hereafter called Galician gneisses) petrographically identical to Castilian gneisses are common.

Given the importance of the precise geochronology of the pre-Arenig magmatism for understanding the pre-Variscan evolution of Iberia, our research group initiated a long term project to date it, having already completed a survey about the Ollo de Sapo Formation (Bea et al. 2006; Montero et al. 2007; Montero et al. 2009). One of the first conclusions that emerged from this survey was that these rocks have an unusually high zircon inheritance (Bea et al. 2007 and references therein), which has complicated extraordinarily dating them using conventional U-Pb on zircon concentrates. This, added to perturbations in the Rb-Sr and Sm-Nd isotopic systems caused by the Variscan deformation and metamorphism, makes mandatory using of single crystal techniques, mainly high resolution ion microprobe U-Pb in zircon, for obtaining accurate crystallization ages.

In this paper we present the results of an extensive zircon U-Pb ion microprobe and LA-ICPMS study focused on both Castilian and Galician metagranitic gneisses, the precise geochronology of which was, for the most part, still poorly known. In total, we have studied 32 gneissic bodies, 22 Castilian and 10 Galician (Figs. 2 and 3). The main objectives were to determine the range of crystallization ages of these rocks and the age populations in the inherited pre-magmatic cores. These data are then compared with the dataset already obtained on other Iberian pre-Arenig rocks and used to constrain the timing of the Cambro-Ordovician magmatism in Central Iberia. Finally, the combination of these data with the ones of other igneous rocks of similar age from the European Variscan Belt enabled us to relate this magmatism with northern margin of Africa during Early Paleozoic.

2. Geological setting and petrography

The Central Iberian and the Galicia Tras-os-Montes Zones (Fig. 1) are located in the internal zone of the Iberian Massif, which is the westernmost part of the European Variscan Belt.

The Central Iberian Zone (see Pérez-Estaún and Bea 2004 and references therein) comprises Late-Proterozoic to Early Paleozoic metasediments, felsic intrusive and extrusive pre-Variscan igneous rocks, and syn- or late-kinematic Variscan granitoids. It is divided into two domains, the small Ollo de Sapo Domain, to the north, mostly composed of the metavolcanic and metagranitic rocks of the Ollo de Sapo Formation, and the large Schist-Graywacke Complex Domain, to the south, characterized by the occurrence of a thick monotonous sequence of Late Proterozoic to Cambrian shales and sandstones with minor conglomerates and limestones.

In the northern part of the Schist-Graywacke Complex Domain, there are abundant pre-Variscan igneous rocks, mostly metagranites and a few metavolcanic rocks, concentrated in four areas: the Tormes Dome, the Anatectic Complex of Toledo, the northern part of the Gredos Sector of the Avila Batholith, and especially Guadarrama, where they form an accumulation of batholithic dimensions (Fig. 2).

The metagranites are mesocratic to leucocratic gneisses, fine-grained or augen, strongly deformed and variably metamorphosed from greenschist to anatexis. They are composed of K-feldspar or, rarely, plagioclase and/or quartz megacrysts embedded in a medium- to coarse-grained groundmass composed of quartz, plagioclase, K-feldspar, biotite and, locally, rare garnet, cordierite, muscovite and sillimanite. Apatite, zircon, monazite, Fe-oxides, xenotime, tourmaline, rutile and sulfides are accessory minerals. Most of these rocks derived from intrusive granites, some of them rapakivi; the only ones which might have derived from a volcanic protolith crop out in the eastern part of the Guadarrama Range, near the La Berzosa fault. The chemical composition of both metagranitic and metavolcanic rocks corresponds to peraluminous, granodioritic to granitic rocks, with $SiO_2 \approx$ 63-77 wt.%, CaO $\approx$ 0.34-1.66 wt.%, $Na_2O \approx$ 1.70-3.99 wt.%, $K_2O \approx$ 3.55-6.37 wt.% and an alumina saturation index (ASI) $\approx$ 1.15-2.07.

The Galicia Tras-os-Montes Zone is located in the northwest of the Iberian Massif and is divided into two domains, Schistose Domain and Allochthonous Complexes (Farias et al. 1987;

Arenas et al. 1988). The former is composed of Paleozoic metasediments, mostly schists, and pre-Variscan and Variscan magmatic rocks, predominately felsic; the latter, that is, the Allochthonous Complexes consist of a superposition of allochthonous units formed of ophiolitic materials with arc and oceanic origin and terrains of continental affinity (Ries and Shackleton 1971; Arenas et al. 1986; Martínez Catalán et al. 1997).

In the Schistose Domain, which supposedly is a tectonic unit placed over the Central Iberian Zone (Arenas et al. 2004 and references therein), there is a roughly curved NW-SE lineament of pre-Variscan metagranites which seem to be a continuation of the NW-SE alignment of igneous rocks of the same age from the northern part of the Schist-Graywacke Complex Domain (Fig. 3). These Galician metagranites are mesocratic to leucocratic rocks, medium- to coarse-grained, all most often with augen textures, always deformed and frequently migmatized. Their mineralogy and textures are nearly identical to the Castilian gneisses. The chemical composition of these gneisses are also equivalent to the Castilian gneisses and corresponds to peraluminous, granodioritic to granitic rocks, with $SiO_2 \approx 65$-76 wt.%, CaO ≈ 0.33-1.28 wt.%, $Na_2O \approx 1.79$-3.96 wt.%, $K_2O \approx 3.89$-6.31 wt.% and an alumina saturation index (ASI) ≈ 0.96-1.6.

3. Samples and methods

For this study we have sampled 22 Castilian gneisses and 10 Galician gneisses (Figs.2 and 3). Zircons from 28 samples were separated using conventional magnetic and heavy-liquid techniques (Table 1). Once mounted and polished, zircon grains were studied by cathodoluminescence imaging using a LEO 1430-VP scanning electronic microscope (SEM) at the Scientific Instrumentation Center (CIC) of the University of Granada. Subsequently they were analyzed for U-Th-Pb using ion microprobe and a Laser Ablation ICP-MS techniques.

Ion microprobe analyses were done in a CAMECA IMS1270 instrument at the NORDSIM facility (Stockholm). Analytical methods broadly follow those described by Whitehouse et al. (1999), Whitehouse and Kamber (2005) and references mentioned therein. U/Pb and Th/Pb ratios were calibrated using the Geostandards 91500 reference zircon (1065 Ma (Wiedenbeck et al. 1995)) and include a propagated error component from replicate analyses of 91500 during the analytical session. Errors on $^{207}Pb/^{206}Pb$ ratios are either the observed analytical uncertainty or the counting statistics error, whichever is highest. Common Pb, as revealed by monitoring ^{204}Pb, was in most cases relatively small and had little influence on the interpreted age. When required, common lead was corrected either using the "207-correction" which is calculated by projecting the uncorrected analyses onto concordia from the assumed common $^{207}Pb/^{206}Pb$ present day composition, and from the measured ^{204}Pb using the $^{204}Pb/^{207}Pb$ ratios provided by the Stacey and Kramers (1975) model at the calculated age. All ages are calculated using the decay constant recommendations of Steiger and Jäger (1977).

LA-ICPMS analyses of Th, U and Pb isotopes were carried out with a Nd-YAG 213 nm Mercantek laser and a torch-shielded quadrupole Agilent 7500 ICP-MS spectrometer. The laser beam was set at a diameter of 60 µm, with a repetition rate of 10 Hz and an output energy of 75%. The ablation time was 60 s and the spot was pre-ablated during 45 s with a laser output energy of 50%. The ablation was done in a He atmosphere. ^{91}Zr was used as an internal standard. The external standard was the NIST-610 glass, which contains 434 ppm Ti, 439.9 ppm Zr, 417.7 ppm Hf, 409 ppm Pb, 457.1 ppm U and 450.6 ppm Th (Pearce et al. 1997). The following isotope ratios, determined by TIMS at the University of Granada, were also used: $^{204}Pb/^{206}Pb$ =

0.06, $^{207}Pb/^{206}Pb = 0.9127$, $^{208}Pb/^{206}Pb = 2.1898$, $^{206}Pb/^{238}U = 0.2501$, $^{208}Pb/^{232}Th = 0.5402$. U-Pb LA-ICPMS ages are in good agreement with ion-microprobe data but show more dispersion and tend to be more discordant. The precision (1σ) estimated on ten replicates of the NIST-610 analyzed in the same run was better than 2.5% for element ratios and ca. 0.3% for isotope ratios. Common lead interferences are significantly higher than in ion microprobe analyses, owing to the larger spot diameter. Data with a discordance factor $(^{206}Pb/^{238}U)age/(^{207}Pb/^{235}U)age < 0.9$ were always rejected, except they plot in a well-defined discordia line. In the rest, common lead was corrected using the same methods as described in the previous section.

Sr and Nd isotopes from 26 samples were analyzed at the CIC of the University of Granada (Table 2). Theses samples (0.1000 g) were digested with HNO_3 + HF in a Teflon-lined vessel and analyzed by thermal ionization mass spectrometry (TIMS) in a Finnigan Mat 262 RPQ spectrometer after separation with ion-exchange resins using conventional procedures. All reagents were ultra clean. Normalization values were $^{86}Sr/^{88}Sr = 0.1194$ and $^{146}Nd/^{144}Nd = 0.7219$. Blanks were 0.6 and 0.09 nanograms for Sr and Nd. The external precision (2σ), estimated by analyzing 10 replicates of the standard WS-E (Govindaraju et al. 1994), was better than ± 0.003% for $^{87}Sr/^{86}Sr$ and ± 0.0015% for $^{143}Nd/^{144}Nd$. $^{87}Rb/^{86}Sr$ and $^{147}Sm/^{144}Nd$ were directly determined by ICP-MS at Granada following the method developed by Montero and Bea (1998), with a precision better than ± 1.2% and ± 0.9% (2σ) respectively. Average values were $^{87}Sr/^{86}Sr = 0.710257$ with SE = 0.0007785% for NBS-987 and $^{143}Nd/^{144}Nd = 0.511851$ with SE = 0.00169% for La Jolla.

4. Sr and Nd isotope composition.

The Sr and Nd isotope composition of the Castilian gneisses is characterized by average values of $(^{87}Sr/^{86}Sr)_{485Ma}$ ≈ 0.712, $(\varepsilon_{Nd})_{485Ma}$ ≈ -4.4 and T_{DM} ≈ 1.63 Ga (Table 2) and is typical of rocks derived from old continental materials. In detail, gneisses of the Tormes Dome and Guadarrama have a slightly more primitive average value of $^{87}Sr/^{86}Sr_{485Ma}$ ≈ 0.712 than gneisses of Gredos with an average of $(^{87}Sr/^{86}Sr)_{485Ma}$ ≈ 0.715. However, last ones have more primitive average values of $(\varepsilon_{Nd})_{485Ma}$ ≈ -4.1 and T_{DM} ≈ 1.52 Ga than the gneisses of the Tormes Dome and Guadarrama with $(\varepsilon_{Nd})_{485Ma}$ ≈ -4.7 and -4.4 and T_{DM} ≈ 1.67 and 1.66 Ga respectively.

The Galician gneisses have a Sr and Nd isotopic composition similar to the Castilian gneisses, with an average composition of $(^{87}Sr/^{86}Sr)_{485Ma}$ ≈ 0.711, $(\varepsilon_{Nd})_{485Ma}$ ≈ -4.71 and T_{DM} ≈ 1.76 Ga, except for the Sisargas gneiss which is more primitive. This gneiss has almost identical $(^{87}Sr/^{86}Sr)_{485Ma}$ ≈ 0.709 but the $(\varepsilon_{Nd})_{485Ma}$ is higher, varying between -0.92 and 0.22, and T_{DM} is younger, ranging from 1.1 to 1.2 Ga.

5. Zircon geochronology

U-Pb zircon data for each massif, including neoformed and inherited zircon, are plotted in a wide-scale Tera-Wasserburg concordia diagrams. The data corresponding to the youngest population, interpreted as the crystallization age, are also displayed in a Wetherill concordia plots. The crystallization ages of every massif are summarized in Table 1. Complete U-Pb data are given in Tables 3 and 4 (Online Resource 1 and 2).

5.1 *Castilian gneisses*

5.1.1 The Tormes Dome

In this area, we sampled three metagranites in the west part of the Zamora and Salamanca provinces: Fermoselle, Vitigudino and Ledesma (Fig 2). Cathodoluminescence imaging revealed the presence of two morphological types: uniform grains with oscillatory magmatic zoning, and composite grains formed of cores overgrown by discordant rims. The later are by far the more abundant, accounting for 74 to 82% of the total. U-Pb ion microprobe dating reveals the following:

In Fermoselle, there is a concordant or nearly concordant population composed of six points, with an average of 486 ± 6 Ma interpreted as the crystallization age (Fig. 4.1A and B). There are three older points at 568, 865 and 973 Ma, and a younger age at approximately 407 Ma which probably represents a mixture with a narrow Variscan overgrowth (Fig. 4.1A).

In Vitigudino, there are two concordant populations (Fig. 4.2A). The younger, and most abundant, found in rims, comprises nine points with a mean age of 489 ± 5 Ma, considered the age of crystallization (Fig. 4.2B); the older population, found in cores, has a mean age of 591 ± 3 Ma. There are also one concordant point at 531 Ma, which probably represents a mixed age between the two populations mentioned above, and another three concordant points, one at 643 Ma and two at 1.0 Ga (Fig. 4.2A).

Finally, the Ledesma metagranite also has two concordant populations (Fig. 4.3A). The youngest, consisted of five points, has a mean age of 471 ± 7 Ma, regarded as the crystallization age of the body (Fig. 4.3B), and the second one has a mean age of 631 ± 21 Ma. There are also two older concordant points at 938 and 1156 Ma (Fig. 4.3A).

In short, the crystallization ages for the three metagranites are 486 ± 6 Ma in Fermoselle, 489

± 5 Ma in Vitigudino and 471 ±7 Ma in Ledesma which is, therefore, significantly younger than the others.

5.1.2. Northern Gredos

In this area, we sampled 3 metagranites: San Pelayo, Castellanos and Bercimuelle (Fig. 2).

San Pelayo has two concordant populations of zircons (Fig. 4.4A). The younger and most abundant, found in rims or uniform grains, is composed of nine points with a mean age of 492 ± 4 Ma, considered as the age of crystallization (Fig. 4.4B). The older population, found in cores, has a mean age of 604 ± 15 Ma. There are also some zircon cores that yielded older ages, one at 717 Ma, one at 912 Ma, four at about 2.0 Ga and one at about 2.6 Ga (Fig. 4.4A). Apart from this, there are younger-than-crystallization ages between 466 and 433 Ma, caused by tiny Variscan overgrowths (Fig. 4.4A).

The Castellanos metagranite has three main concordant populations (Fig. 4.5A). The most abundant includes fourteen points with a mean age of 498 ± 4 Ma regarded as the age of crystallization (Fig. 4.5B). The other two populations have mean ages of 548 ± 10 and 612 ± 10 Ma respectively. There are also 4 older concordant points at 683 and 752 Ma, and 1.8 and 3.2 Ga (Fig. 4.5A).

Zircons from the Bercimuelle metagranite display a highly complex age distribution with four concordant populations (Fig.4.6A). The youngest and most abundant, comprised sixteen points, has a mean age of 488 ± 3 Ma which represents the age of crystallization (Fig. 4.6B). The other three populations, interpreted as inherited, have mean ages of 545 ± 3, 622 ± 12 and 747 ± 18 Ma respectively. Additionally, there are some data clustering around 2.0 Ga, and a discordia line with an upper intersection close to 2.7 Ga (Fig. 4.6A).

It follows, therefore, that the Cambro-Ordovician gneisses of Gredos are older than their equivalents of the Tormes Dome: 492 ± 4 Ma in San Pelayo, 498 ± 4 Ma in Castellanos and 488 ± 3 Ma in Bercimuelle. It is worthy of emphasizing that the Castellanos and Bercimuelle metagranites have a well-defined inherited population at ≈ 545 Ma, the age of the Almohalla orthogneiss and the most frequent inherited age in the migmatites of the neighboring Peña Negra anatectic complex (Bea et al. 2003).

5.1.3. Guadarrama

Since Guadarrama is the largest domain of Cambro-Ordovician rocks in Spain, we studied eight metagranites (La Cañada, La Hoya, La Estación (I and II), mesocratic and leucocratic Vegas de Matute, La Morcuera and Buitrago de Lozoya) and three metavolcanic rocks (La Berzosa, El Cardoso and Riaza) (Fig. 2).

La Cañada metagranite yield two concordant zircon populations (Fig. 5.1A). The first, representing the crystallization age, consists of six points with a mean of 489 ± 9 Ma (Fig. 5.1B); the second, inherited, has a mean age of 571 ± 14 Ma. Moreover, there are two data at about 1.7 and 2.7 Ga and several younger-than-crystallization ages between 338 and 440 Ma approximately, related to Variscan overgrowths (Fig. 5.1A).

La Hoya metagranite has a concordant population, composed of six points, with a mean age of 478 ± 7 Ma which represents the crystallization age (Fig. 5.2B). There are also two isolated subconcordant points at 710 and 393 Ma (Fig. 5.2A).

The slightly deformed coarse-grained facies of La Estación (La Estación I) yield a crystallization age of 490 ± 5 Ma (Fig. 5.3B), calculated from ten nearly concordant points, and a few older ages at ca. 610, 650 and 920 Ma (Fig. 5.3A). The extremely deformed, fine-grained facies (La Estación II), on the other hand, have only a population, consisted of six nearly concordant points, with a mean age of 473 ± 8 Ma (Fig. 5.4A and B). Remarkably, it is one of the few studied Cambro-Ordovician Iberian rocks which little zircon inheritance.

The mesocratic facies of the Vegas de Matute metagranite has two main populations (Fig. 5.5A), one concordant, comprises nine points, with a mean age of 476 ± 5 Ma (Fig. 5.5B), and other subconcordant at 574 ± 17 Ma. Besides, there are also two older points at 1.0 and 2.0 Ga approximately (Fig. 5.5A). The leucocratic facies, on the other hand, has a nearly concordant population composed of thirteen points, with a mean age of 484 ± 6 Ma regarded as its crystallization age (Fig. 5.6B). It also contain some Variscan overgrowths with probably mixed ages between 432 and 365 Ma approximately (Fig. 5.6A).

La Morcuera metagranite contains two nearly concordant populations (Fig. 6.1A). The most abundant one, with six points, has a mean age of 482 ± 8 Ma that represents the age of crystallization of this metagranite (Fig. 6.1B). The second and less abundant one has a mean age of 639 ± 13 Ma. There are also two nearly concordant ages, at 515 and 570 Ma approximately, which probably represent mixed ages between the two populations mentioned above, and another nearly concordant point at about 725 Ma (Fig. 6.1A).

Finally, the U-Pb data of the Buitrago de Lozoya metagranite provide two small concordant populations (Fig. 6.2A). The first, consisting of four points, yields a mean age of 481 ± 9 Ma, considered as the crystallization age of this body (Fig. 6.2B); the second has a mean age of 547 ± 15 Ma. There are also four concordant or nearly concordant older ages at 625, 650 and 840 Ma, and 2.7 Ga approximately (Fig. 6.2A).

Regarding the SIMS U-Pb data of the metavolcanic rocks of Guadarrama, they are detailed as follows:

Zircons from the La Berzosa metavolcanic rocks reveal the presence of two nearly concordant populations (Fig. 6.3A). The first consists of six points with a mean age of 462 ± 11 Ma that represents the crystallization age of these rocks (Fig. 6.3B). The second has a mean age of 613 ± 5 Ma. Moreover, there are three older concordant ages at 690 Ma, 2.0 and 2.7 Ga approximately (Fig. 6.3A).

The metavolcanic rocks of the El Cardoso yield a crystallization age of 483 ± 6 Ma calculated on nine points (Fig. 6.4B). There are also some older subconcordant points at 599, 609, 658 and 870 Ma and a discordant point near 2.0 Ga (Fig. 6.4A). Apart from this, there is a Variscan overgrowth at 321 Ma (Fig. 6.4A).

Finally, the U-Pb data of the Riaza metavolcanic rocks reveal the existence of three concordant populations (Fig. 6.5A). One is composed of six points with a mean age of 475 ± 5 Ma which represents the crystallization age of these rocks (Fig. 6.5B), and the other two populations have mean ages of 545 ± 11 and 599 ± 6 Ma. There are three older nearly concordant ages two at 639 and 643 Ma, and at 2.0 Ga (Fig. 6.5A).

To sum up, Cambro-Ordovician gneisses of Guardarrama are slightly younger than the analogs of Gredos: 490 ± 5 in La Estación I, 489 ± 9 in La Cañada, 484 ± 6 in Vegas de Matute (leucocratic), 483 ± 6 in El Cardoso, 482 ± 8 in La Morcuera, 481 ± 9 in Buitrago de Lozoya, 478 ± 7 in La Hoya, 476 ± 5 in Vegas de Matute (melanocratic), 475 ± 5 in Riaza, 473 ± 8 in La

Estación II and 462 ± 11 Ma in La Berzosa. Furthermore, these gneisses have a high proportion of inherited cores which cluster around three well-defined populations at ~545 Ma, ~575 and ~605 Ma. The first one has been also found in the gneisses of Gredos but the other two are observed for the first time in the Cambro-Ordovician igneous rocks from Central Iberia. The ~575 Ma population approximately correspond to the crystallization ages of Aljucén and Mérida mafic rocks (Bandrés et al. 2004; Talavera et al. 2008). The other population at ~605 Ma does not fit the crystallization age of any igneous body from Central Spain but has been described in the Ollo de Sapo Formation as an inherited population (Montero et al. 2007; Montero et al. 2009).

5.1.3 Anatectic Complex of Toledo

In the north of the Anatectic Complex of Toledo, we sampled two metagranites, Polán and Mohares (Fig. 2). Cathodoluminescence images showed uniform grains, with magmatic oscillatory zoning, and grains with inherited cores in which percentage ranges between 76 and 80%. SIMS U-Pb data reveal the following:

In Polán, there is a concordant population of six points with a mean age of 480 ± 8 Ma considered, therefore, as the crystallization age (Fig. 6.6B); there are also two older concordant points at 521 and 587 Ma and one younger-than-crystallization age at 429 Ma caused by a tiny Variscan overgrowth (Fig. 6.6A).

The Mohares metagranite contains very little zircons. We analyzed just four uniform grains that yielded a mean age of 489 ± 7 Ma considered, therefore, the age of crystallization of this body (Fig. 7A and B).

5.2 *Galician gneisses*

In the Schistose Domain of the Galicia Tras-os-Montes Zone, we sampled nine metagranites: Cherpa, Noia, Laxe, Pontevedra, Vilanova, Bangueses, Bande, Rial de Sabucedo and San Mamede (Fig. 3). Zircons from these metagranites are either uniform with magmatic oscillatory zoning, or composed of a magmatic rim and a pre-magmatic core. The percentage of grains with inherited cores ranges between 25 and 55%.

In the Cherpa metagranite, sixteen concordant points define a population with a mean of 470 ± 6 Ma, considered as the crystallization age (Fig. 8.1B). Besides, there are older ages at 558 and 630 Ma, two points at about 2.0 Ga and a discordia line with an upper intersection at 2.45 Ga (Fig. 8.1A). Finally, there are younger-than-crystallization ages between 447 and 367 Ma, caused by Variscan overgrowths (Fig. 8.1A).

In the Noia metagranite, there are nineteen concordant points with a mean age of 481 ± 5 Ma that we regard as the age of crystallization (Fig. 8.2B). Besides this, there are older ages at 525, 591 and 612 Ma, two points at about 1.0 Ga and one point at about 2.0 Ga (Fig. 8.2A).

The Laxe metagranite has two nearly concordant populations (Fig. 8.3A). The youngest and most abundant comprises sixteen points with a mean age of 497 ± 6 Ma, considered as the crystallization age (Fig. 8.3B). The other population, less abundant, has a mean age of 608 ± 9 Ma. There are also a few older points at 649, 651, 654, 677 and 713 Ma, and a discordia line with an upper intersection at 2.6 Ga (Fig. 8.3A). Finally, there are also younger-than-crystallization ages between 398 and 461 Ma (Fig. 8.3A).

The Pontevedra metagranite has a concordant population of fifteen points with a mean age of

475 ± 6 Ma, considered as the age of crystallization (Fig. 8.4B). Besides this, there are older ages at 515, 546, 568 and 596 Ma and a discordia line with an upper intersection at 2.65 Ga (Fig. 8.4A). Eventually, there are also younger-than-crystallization ages between 441 and 425 Ma (Fig. 8.4A).

In the Vilanova metagranite, the youngest population comprises seven points with a mean age of 476 ± 9 Ma, regarded as the crystallization age (Fig. 8.5B). The oldest population is less abundant, with a mean age of 541 ± 10 Ma. Additionally, there are a discordia line with an upper intersection at 2.1 Ga, and younger-than-crystallization ages between 437 and 394 Ma (Fig. 8.5A).

The U-Pb LA-ICPMS and SIMS data of the Bangueses metagranite show a concordant population comprising ten points with a mean age of 482 ± 7 Ma, considered as the age of crystallization (Fig. 8.6B). Besides this, there are three older ages at 519, 562 and 932 Ma and a discordia line with an upper intersection at ca. 1.9 Ga (Fig. 8.6A). Finally, there are also younger-than-crystallization ages between 448 and 394 Ma (Fig. 8.6A).

The Bande metagranite display a nearly concordant population composed of eight points with a mean age of 462 ± 8 Ma, considered the crystallization age of this body (Fig. 9.1B). There are also older ages at about 1.0 Ga and a discordia line with an upper intersection at 2.3 Ga approximately, and a few younger-than-crystallization ages between 442 and 329 Ma caused by Variscan overgrowths (Fig. 9.1A).

The Rial de Sabucedo metagranite shows two nearly concordant populations (Fig. 9.2A). The youngest and most abundant one comprises ten points with a mean age of 480 ± 10 Ma, considered as the age of crystallization (Fig. 9.2B). The less abundant population has a mean age of 576 ± 12 Ma. Besides these, there are five older ages at 631, 632, 657 and 766 Ma, and ca. 2.85 Ga and a discordia line with an upper at 2.3 Ga (Fig. 9.2A).

Finally, the San Mamede metagranite has two nearly concordant populations (Fig. 9.3A). The youngest and most abundant comprises nineteen points with a mean age of 486 ± 8 Ma, considered as the crystallization age of this metagranite (Fig. 9.3B). The second, and less abundant, clusters around 595 ± 8 Ma. There are also a considerable number of older ages which are at 675, 682, 747, 777, 801 and 940 Ma, two points at 1.0 Ga, and other three older ages at 2.0, 2.1 and 2.5 Ga (Fig. 9.3A), plus two discordia lines with upper intersections at ca 2.3 Ga and ca 2.6 Ga (Fig. 9.3A). Finally, there are four younger-than-crystallization ages between 434 and 380 Ma caused by Variscan overgrowths (Fig. 9.3A).

To summarize, the crystallization ages of the Galician gneisses are equivalent to the ones of Castilian gneisses and they are: 497 ± 6 in Laxe, 486 ± 8 in San Mamede, 482 ± 7 in Bangueses, 481 ± 5 in Noia, 480 ± 10 in Rial de Sabucedo, 476 ± 9 in Vilanova, 475 ± 6 in Pontevedra, 470 ± 6 in Cherpa and 462 ± 8 Ma in Bande. These gneisses also have three inherited populations at ~545, ~575 and ~605 Ma similar to the ones of the Castilian gneisses.

6 . Discussion

6.1 Age and nature of this magmatism

Our data reveal that the Cambro-Ordovician magmatism of the northern part of the Schist-Graywacke Complex Domain and the Schistose Domain of the Galicia Tras-os-Montes Zone is coeval. It took place between 498 Ma to 462 Ma, with the magmatic activity peaking at 485 Ma and 480 Ma respectively. The Table 1 summarizes the estimated crystallization ages of all studied bodies. According to the cathodoluminescence imaging and U-Pb data, zircons from the Cambro-Ordovician rocks of the two domains have an elevated percentage of inherited cores, between 52% and 94% in the Castilian gneisses, and between 25% and 55% in the Galician gneisses (Fig. 10).

The main part of inherited zircons are Ediacaran. These form three populations with mean ages at 545 ± 3, 575 ± 4 and 611 ± 5 Ma in the Castilian gneisses, and 545 ± 6, 578 ± 5 and 607 ± 5 Ma in the Galician gneisses, identical within errors (Fig. 11). Both groups of gneisses also have similar populations of older-than-Ediacaran inherited ages, being recognizable Cryogenian (650-700 Ma), Tonian (850-1000 Ma), Mesoproterozoic (1.0-1.2 Ga), Orosirian (1.9-2.0 Ga), Neoarchean (2.5-2.6 Ga) zircons (Fig. 11). In Castellanos metagranite from Northern Gredos, we also found an inherited core of Mesoarchean age (3.2 Ga) (Fig. 11).

Besides the closely similar crystallization age and virtually identical distribution of the age of inherited zircon components, the metagranites and metavolcanic rocks of both areas also have almost the same average isotopic composition. The average values for the Castilian metagranites and metavolcanic rocks are $T_{DM} \approx 1.63$ Ga, $(\varepsilon_{Nd})_{485Ma} \approx -4.4$, and $(^{87}Sr/^{86}Sr)_{485Ma} \approx 0.712$, whereas for the Galician metagranites are $T_{DM} \approx 1.76$ Ga, $(\varepsilon_{Nd})_{485Ma} \approx -4.71$ (except for the Sisargas orthogneiss, which is slightly more primitive), and $(^{87}Sr/^{86}Sr)_{485Ma} \approx 0.711$, virtually identical, therefore. This points out that the source rocks of the Cambro-Ordovician magmas in the Schist-Graywacke Complex Domain and the Schistose Domain of Galicia Tras-os-Montes Zone was similar.

Based on lithological and tectonometamorphic similarities between the Schistose Domain of Galicia Tras-os-Montes Zone and Central Iberian Zone, Arenas et al. (2004) proposed that the Schistose Domain had not been strongly displaced from its original position, and consequently, would not be an allochthonous terrane but a tectonic unit. Our data confirm this opinion because the identical age and isotope signature indicates that the Cambro-Ordovician magmatism of the two areas derived from a similar source.

6.2 Comparison with the Cambro-Ordovician magmatism of other zones of the Central Iberian Zone and European Variscan Belt

The Central Iberian Zone contains three other lineaments of Cambro-Ordovician igneous rocks (Fig. 1). To the north, near the boundary with the Western Asturian-Leonian Zone, the Ollo de Sapo Formation. To the south, near the boundary with the Ossa Morena Zone, the Urra Formation and Portalegre and Carrascal granitoids. In the middle-south, the plutons of Oledo (Antunes et al. 2009), Gouveia (Neiva et al. 2009) and Zarza (Corretgé et al. pers. com.), which, in contrast with the rest of Iberian Cambro-Ordovician Rocks, comprise undeformed, or slightly deformed, granitoids previously interpreted as Variscan.

The magmatism in the Ollo de Sapo and the Urra formations peaked at 490 Ma (Sola et al. 2006; Bea et al. 2006; Montero et al. 2007; Sola et al. 2008; Montero et al. 2009), slightly before than in the two areas studied here (480- 485 Ma) and also contains an abnormally high fraction of zircons with inherited cores (see Bea et al. (2007) and references therein). The distribution of inherited ages, however, is slightly different (Fig. 12). Whereas the Ollo de Sapo and Urra formations have just one Ediacaran population at 600-610 Ma, the Castilian and Galician gneisses show three distinctive Ediacaran-Early Cambrian populations at 540-550, 575-585 and 605-615 Ma (Fig 12). The Nd isotope composition is also slightly more primitive (Fig. 13), with an average T_{DM} = 1.41 Ga and $(\varepsilon_{Nd})_{485Ma}$ = -2.7 . It seems therefore that the source rocks, despite the same Pan-African linkage, was slightly different.

Despite the scarcity of data about the undeformed Cambro-Ordovician granitoids of the Gouveia-Oledo-Zarza lineation, they seem to be different from the rest of the Iberian Cambro-Ordovician magmatic rocks. Antunes et al. (2009) and Neiva et al. (2009) have studied the Portuguese granitoids founding that the zircon inheritance is small, and that the Nd and Sr isotope composition is notably more primitive (Fig 13). Certainly, more studies are required to place properly these rocks within the framework of the Cambro-Ordovician magmatism of Iberia.

Rocks similar to the ones described here are found all over the European Variscan Belt, where a large volume of granodioritic-granitic intrusions and metavolcanic rocks was generated between 510 and 470 Ma. As in Iberia, these rocks have an important zircon inheritance with an age distribution ranging from 540 Ma to 2.9 Ga (Fig. 14 and references therein) with the following distribution: three Ediacaran-Early Cambrian (530-540, 570-580 and 610-620 Ma) and one Orosirian (1.9-2.0Ga) (Fig. 14). There are also an important percentage of Cryogenian and Tonian ages with a wide range of ages (Fig. 14). Apart from this, there are also some Mesoproterozoic (1.0-1.25 Ga) and Neo- (2.5-2.7Ga) and Mesoarchean (2.9 Ga) ages (Fig. 14).

It is clear, therefore, that about 65% of pre-magmatic cores of these rocks are Ediacaran-Early Cambrian, thus suggesting that the protolith of the European Cambro-Ordovician magmatism was mostly composed of Panafrican igneous rocks, as in Iberia (Fig. 15). This hypothesis is supported by the Sr-Nd isotopes of Panafrican igneous rocks from the European Variscan Belt (Mérida, Iberian Massif (Bandrés et al. 2004), Saxo-Thuringian Zone, Bohemian Massif (Kroner et al. 1994; Kroner et al. 1995; Tichomirowa et al. 2001; Linnemann and Romer 2002)). The Sr-Nd isotopic composition of these rocks, recalculated to 485 Ma, is similar to the one of the Cambro-Ordovician rocks (Fig. 16), with average isotopic composition of $(^{87}Sr/^{86}Sr)_{485Ma} \approx 0.710$ and 0.709, $(\varepsilon_{Nd})_{485Ma} \approx -5.0$ and -3.5, $T_{DM} \approx 1.59$ and 1.58 Ma respectively, and would indicate that Cambro-Ordovician magmas would have been generated by partial melting of Panafrican rocks similar to Europe with no significant contribution of mafic magmas except in some rocks from Black Forest and Central Iberian Zone.

The remaining 35% of inherited cores points out to the existence of an older-than Ediacaran crust which could have also been present in the source of the Cambro-Ordovician magmas from the European Variscides. This contribution is also suggested by the fact that Nd model ages (T_{DM}) of these igneous rocks peak at 1.45-1.55 Ga (Fig. 17 and references therein). This age has been interpreted as a proof of the involvement of a Mesoproterozoic crust, as main source, in the generation of the Cambro-Ordovician magmas by Fernández-Suárez et al. (2000) and Murphy et al. (2008). However, the almost universal simultaneous occurrence of Ediacaran to Paleoproterozoic inherited zircons rejects that idea and suggest that the 1.5 Ga Nd model age would be the result of the mixture of different components.

The Cambro-Ordovician magmatism of the European Variscan Belt has been related during the last decade to the opening of the Rheic ocean in the Early Paleozoic caused by the detachment of several Neoproterozoic arc terranes from the continental margin of northern Gondwana (Nance et al. 2010). These terranes, called Cadomia, have been supposed to be attached to the West African Craton, considered the only possible source for the Archean components (Nance et al. 2010). Nevertheless, recent U-Pb dating on zircons from Tuareg Shield (Algeria) (Henry et al. 2009; Fezaa et al. 2010), Western Egypt (Bea et al. 2010; Bea et al. 2011) and North-Central Sudan (Kuster et al. 2008) have revealed the presence of Panafrican and Archean igneous rocks in the central-eastern part of north Africa, in the region known as the Saharan Metacraton (Abdelsalam et al. 2002). Hence, a comparison between Panafrican igneous rocks from West African Craton and Saharan Metacraton and Cambro-Ordovician igneous rocks from European Variscan Belt is essential. From the comparison of all available geochronological and isotopic data of these rocks, some similarities are distinguished.

On the one hand, Panafrican rocks from West African Craton show crystallization ages, from 532 to 625 Ma, with two main peaks at 545-550 and 610-615 Ma (Fig. 15) (Compston et al. 1992; Walsh et al. 2002; Gasquet et al. 2004; Gasquet et al. 2005; Eddif et al. 2007; Pouclet et al. 2008; El Hadi et al. 2010), similar to Ediacaran-Early Cambrian inherited populations of the European Cambro-Ordovician igneous rocks. The Sr-Nd isotopic composition of these Panafrican rocks are also comparable to the last ones (Fig. 16), with an average $(^{87}Sr/^{86}Sr)_{485Ma} \approx$ 0.708 and a $(\varepsilon_{Nd})_{485Ma} \approx$ -3.4 (Gasquet et al. 2005; Barbey et al. 2001). However, zircon inheritance of these rocks are scarce, with only a few pre magmatic cores at 700 Ma and 1.8 and 2.2 Ga (Fig. 15), and Nd model ages (T_{DM}) are younger, with a peak at 1.15-1.25 Ga (Fig. 17).

On the other hand, Panafrican rocks from Saharan Metacraton also display crystallization ages, from 555 to 615 Ma, with two main peaks at 555-560 and 610-615 Ma (Fig. 15) (Kuster et al. 2008; Henry et al. 2009; Bea et al. 2010; Fezaa et al. 2010), equivalent to Ediacaran-Early Cambrian inherited populations of the Cambro-Ordovician igneous rocks from Europe.

Furthermore, the Sr isotopic composition of these rocks is similar to the European Cambro-Ordovician igneous rocks, with an average $(^{87}Sr/^{86}Sr)_{485Ma} \approx 0.709$, but Nd isotopic composition is slightly different, with $(\varepsilon_{Nd})_{485Ma}$ between -11.8 to 2.2 (Kuster et al. 2008; Bea et al. 2010; Fezaa et al. 2010), these being indistinguishable from the values of $(\varepsilon_{Nd})_{485Ma}$ of the Panafrican igneous rocks from the Iberian and Bohemian massifs (Fig. 16). Moreover, these Panafrican rocks have a significant zircon inheritance, composed of Cryogenian, Tonian, Mesoproterozoic, Orosirian and Archean cores (Fig. 15), and Nd model ages (T_{DM}) with a peak at 1.45-1.55 Ga (Fig. 17).

It is evident that Panafrican igneous rocks from West African Craton and Saharan Metacraton have comparable geochronological and Sr-Nd isotope features. Rocks from both areas have almost identical average $(^{87}Sr/^{86}Sr)_{485Ma}$, 0.708 and 0.709 respectively, and crystallization ages, with two peaks at 545-555 and 605-615 Ma. However, the distribution of inherited zircon ages and Nd model ages of these rocks are remarkably different. The range of inherited zircon ages of the Panafrican igneous rocks from Saharan Metacraton is wider and includes Mesoproterozoic and Archean cores, absent in the West African Craton, and the average values of Nd model ages are older, $T_{DM} \approx 1.45\text{-}1.55$ Ga. The above data of the Panafrican igneous rocks from Saharan Metacraton match better with the zircon inheritance and Nd model ages of the Cambro-Ordovician igneous rocks from the European Variscan Belt. Hence, it may be concluded that Cadomia would be attached to Saharan Metacraton during Early Paleozoic. This hypothesis is in agreement with Hf data of granulites zircons from Central Iberian Zone (Villaseca et al., 2011) and the palaeogeographic reconstructions of NW Iberia for Lower Paleozoic times (Gutiérrez-Marco et al., 2002). Hf isotopic data in granulite zircons show a cryptic presence of a minor

Mesoproterozoic mantle input at 1.0-1.2 Ga in the granulite-facies rocks from central Spain that coincides with a crustal generation events in central Africa at 1.0-1.3 Ga (Villaseca et al., 2011). Moreover, the palaeographic reconstructions, based on benthic faunas, indicate that NW Iberia would have be located near the Algerian Sahara or Libya during Lower Paleozoic (Gutiérrez-Marco et al., 2002).

7. Summary and conclusions

The main conclusions of this work can be summarized as follows:

The Cambro-Ordovician magmatism from the northern part of the Schist-Graywacke Complex Domain and the Schistose Domain of Galicia Tras-os-Montes Zone occurred almost at the same time. This magmatism started at 498 Ma, reached a maximum at 485 in the Castilian gneisses and 480 in the Galician gneisses, and ceased at 462 Ma.

This magmatism is characterized by an important zircon inheritance, ranging from 54% to 94% in the Castilian gneisses and from 25% to 55% in the Galician gneisses. Most of these pre-magmatic cores are Ediacaran-Early Cambrian which mainly cluster around three well-defined populations at 545-550, 575-580 and 605-610 Ma. Minor Cryogenian (650-700 Ma), Tonian (850-1000 Ma), Orosirian (1.9-2.0 Ga), Mesoproterozoic (1.0-1.2 Ga) and Neo- (2.5-2.6 Ga) and Mesoarchean (3.2 Ga) cores are also found.

The Sr-Nd isotope composition of the Castilian and Galician gneisses is almost identical with an average of $(^{87}Sr/^{86}Sr)_{485Ma} \approx 0.712$ and 0.711, $(\varepsilon_{Nd})_{485Ma} \approx -4.4$ and -4.71, and $T_{DM} \approx 1.63$ and 1.76 Ga respectively. This composition is typical of rocks derived from old continental materials except for the Sisargas gneiss which has a more primitive isotopic composition with values of

$^{87}Sr/^{86}Sr_{485Ma} \approx 0.709$, $(\varepsilon_{Nd})_{485Ma} \approx -0.99$ to 0.22, and $T_{DM} \approx 1.1$-1.2 Ga.

The zircon inheritance and Sr-Nd isotope composition of the Castilian and Galician gneisses are slightly different from the rest of the Cambro-Ordovician igneous rocks from Central Iberia. Ollo de Sapo and Urra formations, located in the north and south edges respectively, have only one Ediacaran population of inherited cores at 600-610 Ma and a more primitive Sr-Nd isotope composition, with an average $(\varepsilon_{Nd})_{485Ma} = -2.7$ and $T_{DM} = 1.41$ Ga (Sola et al. 2006; Bea et al. 2006; Montero et al. 2007; Sola et al. 2008; Montero et al. 2009). The Gouveia-Oledo-Zarza granitoids, located in the middle-south, has a very small zircon inheritance and a more primitive Sr-Nd isotope composition (Antunes et al. 2009; Neiva et al. 2009). Despite these differences, most of the Cambro-Ordovician igneous rocks from central and NW Iberia seems to have an important Ediacaran component which suggests that the protolith of these igneous rocks was mainly composed of Panafrican rocks.

Cambro-Ordovician magmatism is widespread in the European Variscan Belt and has similar features to the one of Central and NW Iberia. The zircon inheritance is also very high and mostly gathers in three population at 539, 575 and 612 Ma. Minor Meso- and Paleoproterozoic and Neo- and Mesoarchean cores are also present. Furthermore, the Sr-Nd isotope composition is characterized by an average of $(^{87}Sr/^{86}Sr)_{485Ma} \approx 0.709$, $(\varepsilon_{Nd})_{485Ma} \approx -3.5$, $T_{DM} \approx 1.58$ Ma. The similar zircon inheritance and isotopic composition of the Cambro-Ordovician igneous rocks from central and NW Iberia and the rest of the European Variscan Belt indicate that this magmatism was generated by the melting of Ediacaran-Early Cambrian rocks, and minor older-than-Ediacaran rocks, with no significant contribution of mafic magmas except for some igneous rocks from Iberian Massif and Black Forest.

The comparison between Cambro-Ordovician igneous rocks from the European Variscan Belt and Panafrican igneous rocks from West African Craton and Saharan Metacraton suggest that the zircon inheritance, with Meso- and Paleoproterozoic and Archean cores, and Nd model ages, with a peak at 1.45-1.55 Ga, of the Panafrican igneous rocks from Saharan Metacraton match better with the ones of the European Cambro-Ordovician igneous rocks. Therefore, it may conclude that Cadomia, or Neoproterozoic arc terranes from Northern Gondwana, was attached to Saharan Metacraton during Early Paleozoic.

Acknowledgments

We are indebted to S. Pla and E. Artigot for their assistance with collecting samples and to M. Moazzen, U. Linnemann and a third anonymous reviewer for their revision of the early version of the manuscript. This work was financially supported by the Spanish grant CGL2008-02864 and the Andalusian grant RNM1595. The NORDSIM facility is operated under an agreement between the research funding agencies of Denmark, Norway and Sweden, the Geological Survey of Finland and the Swedish Museum of Natural History. This is Nordsim publication number 296.

References

Abdelsalam MG, Liegeois JP, Stern RJ (2002) The Saharan Metacraton. J Afr Earth Sci 34: 119–136

Alexandre P (2007) U-Pb zircon SIMS ages from the French Massif Central and implication for the pre-Variscan tectonic evolution in Western Europe. C R Geosci 339: 613–621

Alvaro M, Apalategui O, Baena J, Balcells R, Barnolas A, Barrera JL, Bellido F, Cueto LA, Díaz de Neira A, Elízaga E, Fernández-Gianotti JR, Ferreiro E, Gabaldón V, García-Sansegundo J, Gómez JA, Heredia N, Hernández-Urroz J, Hernández-Samaniego A, Lendínez A, Leyva F, López-Olmedo FL, Lorenzo S, Martín L, Martín D, Martín-Serrano A, Matas J, Monterserín V, Nozal F, Olive A, Ortega E, Piles E, Ramírez JI, Robador A, Roldán F, Rodríguez LR, Ruiz P, Ruiz MT, Sánchez-Carretero R, Teixell A (1994) Mapa geológico de la Península Ibérica, Baleares y Canarias. Escala 1:1.000.000. ITG-17

Antunes IMHR, Neiva AMR, Silva MMVG, Corfu F (2009) The genesis of I- and S-type granitoid rocks of the Early Ordovician Oledo pluton, Central Iberian Zone (central Portugal). Lithos 111: 168–185

Arenas R, Gil Ibarguchi L, González Lodeiro F, Klein E, Martínez Catalán JR, Ortega Gironés E, Pablo Maciá, JG. de, Peinado M (1986) Tectonostratigraphic units in the complexes with mafic and related rocks of the NW of the Iberian Massif. Hercynica 2: 87–110

Arenas R, Farias P, Gallastegui G, Gil Ibarguchi L, González Lodeiro F, Klein E, Marquínez J, Martín Parra LM, Martínez Catalán JR, Ortega E, Pablo Maciá JG de, Peinado M, Rodríguez-Fernández LR (1988) Características geológicas y significado de los dominios que componen la Zona de Galicia-Tras-os-Montes. II Congreso Geológico de España, Simposios

Arenas R, Martínez Catalán JR, Díaz García F (2004). Zona de Galicia-Tras-os-Montes. In: Vera JA (ed.) Geología de España, 1st edn. Madrid, pp 133–165

Bandrés A, Eguíluz L, Pin C, Paquette JL, Ordóñez B, Le Févre B, Ortega LA, Gil Ibarguchi I (2004) The northern Ossa-Morena Cadomian batholith (Iberian Massif): magmatic arc origin and early evolution. Int J Earth Sci 93: 860–885

Barbey P, Nachit H, Pons J (2001) Magma-host interactions during differentiation and emplacement of a shallow-level, zoned granitic pluton (Tarcouate pluton, Morocco): implications for magma emplacement. Lithos 58: 125–143

Bea F, Montero P, Zinger T (2003) The Nature and Origin of the Granite Source Layer of Central Iberia: Evidence from Trace Element, Sr and Nd Isotopes, and Zircon Age Patterns. J Geol 111: 579–595

Bea F, Montero P, Talavera C, Zinger T (2006) A revised Ordovician age for the oldest magmatism of Central Iberia: U-Pb ion microprobe and LA-ICPMS dating of the Miranda do Douro orthogneiss. Geol Acta 4: 395–401

Bea F, Montero P, Gonzalez Lodeiro F, Talavera C (2007) Zircon inheritance reveals exceptionally fast crustal magma generation processes in Central Iberia during the Cambro-Ordovician. J Petrol 48: 2327–2339

Bea F, Montero P, Talavera C, Abu Anbar MM, Scarrow JH, Molina JF, Moreno JA (2010) The paleogeographic position of Central Iberia in Gondwana during the Ordovician: evidence from zircon chronology and Nd isotopes. Terra Nova 22: 341–346

Bea F, Montero P, Abu Anbar M, Talavera C (2011) SHRIMP dating and Nd isotope geology of the Archean terranes of the Uweinat-Kamil inlier, Egypt-Sudan-Libya. Precambrian Res 189: 328–346

Bertrand MJ, Guillot F, Leterrier J (2000) Age Paléozoïque inférieur (U-Pb sur zircon) de métagranophyres de la nappe du Grand-Saint-Bernard (zona interna, vallée d'Aoste, Italie).

Comptes Rendus de l'Académie des Sciences - Series IIA - Earth and Planetary Science 330: 473–478

Castiñeiras P, Navidad M, Liesa M, Carreras J, Casas JM (2008) U-Pb zircon ages (SHRIMP) for Cadomian and Early Ordovician magmatism in the Eastern Pyrenees: New insights into the pre-Variscan evolution of the northern Gondwana margin. Tectonophysics 461: 228–239

Chen F, Satir M, Ji J, Zhong D (2002) Nd-Sr-Pb isotopes of Tengchong Cenozoic volcanic rocks from western Yunnan, China: evidence for an enriched-mantle source. J Asian Earth Sci 21: 39–45

Compston W, Williams IS, Kirschvink JL, Zichao Z, Guogan MA (1992) Zircon U-Pb ages for the Early Cambrian Time-Scale. J Geol Soc London 149: 171–184

Deloule E, Alexandrov P, Cheilletz A, Laumonier B, Barbey P (2002) In-situ U-Pb zircon ages for Early Ordovician magmatism in the eastern Pyrenees, France: the Canigou orthogneisses. Int J Earth Sci 91: 398–405

Díez Montes A, Martínez Catalán JR, Bellido Mulas F (2010) Role of the Ollo de Sapo massive felsic volcanism of NW Iberia in the Early Ordovician dinamics of northern Gondwana. Gondwana Res 17: 363–376

Drost K, Linnemann U, McNaughton N, Fatka O, Kraft P, Gehmlich M, Tonk C, Marek J (2004) New data on the Neoproterozoic - Cambrian geotectonic setting of the Tepla-Barrandian volcano-sedimentary successions: geochemistry, U-Pb zircon ages, and provenance (Bohemian Massif, Czech Republic). Int J Earth Sci 93: 742–757

Eddif A, Gasquet D, Hoepffner C, Levresse G (2007) Age of the wirgane granodiorite intrusions (Western High-Atlas, Morocco): New U-Pb constraints. J Afr Earth Sci 47: 227–231

El Hadi H, Simancas JF, Martinez-Poyatos D, Azor A, Tahiri A, Montero P, Fanning CM, Bea F, Gonzalez-Lodeiro F (2010) Structural and geochronological constraints on the evolution of the Bou Azzer Neoproterozoic ophiolite (Anti-Atlas, Morocco). Precambrian Res 182: 1–14

Farias P, Gallastegui G, González-Lodeiro F, Marquínez J, Martín-Parra LM, Martínez Catalán JR, de Pablo Maciá JG, Rodríguez Fernández LR (1987) Aportaciones al conocimiento de la litoestratigrafía y estructura de Galicia Central. Memorias Mus. Lab. Mineral. e Geol., Fac. Ciências, Univ. Porto 1: 411–431

Fernández-Suárez J, Gutiérrez-Alonso G, Jenner GA, Turbrett M (2000) New ideas on the Proterozoic-Early Paleozoic evolution of NW Iberia: insights from U-Pb detrital zircon ages. Precambrian Res 102: 185–206

Fezaa N, Liegeois JP, Abdallah N, Cherfouh E, De Waele B, Bruguier O, Ouabadi A (2010) Late Ediacaran geological evolution (575-555 Ma) of the Djanet Terrane, Eastern Hoggar, Algeria, evidence for a Murzukian intracontinental episode. Precambrian Res 180: 299-327

Friedl G, Finger F, Paquette JL, von Quadt A, McNaughton NJ, Fletcher IR (2004) Pre-Variscan geological events in the Austrian part of the Bohemian Massif deduced from U-Pb zircon ages. Int J Earth Sci 93: 802–823

Gasquet D, Chevremont P, Baudin T, Chalot-Prat F, Guerrot C, Cocherie A, Roger J, Hassenforder B, Cheilletz A (2004) Polycyclic magmatism in the Tagragra d'Akka and Kerdous Tafeltast inliers (Western Anti-Atlas Morocco). J Afr Earth Sci 39: 267–275

Gasquet D, Levresse G, Cheillez A, Azizi-Samir MR, Mouttaqi A (2005) Contribution to a geodynamic reconstruction of the Anti-Atlas Morocco) during Pan-African times with the emphasis on inversion tectonics and metallogenic activity at the Precambrian-Cambrian transition. Precambrian Res 140: 157–182

Giacomini F, Bomparola RM, Ghezzo C, Guldbransen H (2006) The geodynamic evolution of the Southern European Variscides: constraints from the U/Pb geochronology and geochemistry of the lower Palaeozoic magmatic-sedimentary sequences of Sardinia (Italy). Contrib Mineral Petr 152: 19–42

Govindaraju K, Potts PJ, Webb PC, Watson JS (1994) 1994 Report on Whin Sill Dolerite WS-E from England and Pitscurrie Micrograbbro PM-S from Scotland: assessment by one hundred and four international laboratories. Geostandards Newsletters XVIII: 211

Guillot F, Schaltegger U, Bertrand JM, Deloule E, Baudin T (2002) Zircon U-Pb geochronology of Ordovician magmatism in the polycyclic Ruitor Massif (internal W Alps). Int J Earth Sci 91: 964–978

Gutiérrez-Marco, J.C., Robardet, M., Rábano, I., Sarmiento, G.N., San José Lancha, M.A., Herranz, P., Pieren, A.P., 2002. Ordovician. In: Gibbons, W., Moreno, T. (eds). The Geology of Spain. The Geological Society of London, pp 31–49

Hasalova P, Janousek V, Schulmann K, Stipska P, Erban V (2008) From orthogneiss to migmatite: Geochemical assessment of the melt infiltration model in the Gfohl Unit (Moldanubian Zone, Bohemian Massif). Lithos 102: 508–537

Helbing H, Tiepolo M (2005) Age determination of Ordovician magmatism in NE Sardinia and its bearing on Variscan basement evolution. J Geol Soc London 162: 689–700

Henry B, Liegeois JP, Nouar O, Derder MEM, Bayou B, Bruguier O, Ouabadi A, Belhai D, Amenna M, Hemmi A, Ayache M (2009) Repeated granitoid intrusions during the Neoproterozoic along the western boundary of the Saharan metacraton, Eastern Hoggar, Tuareg shield, Algeria: An AMS and U-Pb zircon age study. Tectonophysics 474: 417–434

Kroner A, Hegner E, Hammer J, Haase G, Bielicki KH, Krauss M, Eidam J (1994) Geochronology and Nd-Sr systematics of Lusatian granitoids-significance for the evolution of the Variscan Orogen in East-Central-Europe. Geol Rundsch 83: 357–376

Kroner A, Willner AP, Hegner E, Frischbutter A, Hofmann J, Bergner R (1995) Latest Precambrian (Cadomian) zircon ages, Nd isotopic systematics and P-T evolution of granitoid orthogneisses of the Erzgebirge, Saxony and Czech-Republic. Geol Rundsch 84: 437–456

Kroner A, Hegner E (1998) Geochemistry, single zircon ages and Sm-Nd systematics of granitoid rocks from the Gory Sowie (Owl Mts), Polish west Sudetes: evidence for early Palaeozoic arc-related plutonism. J Geol Soc London 155: 711–724

Kroner A, Jaeckel P, Hegner E, Opletal M (2001) Single zircon ages and whole rock Nd isotopic systematics of early Palaeozoic granitoid gneisses from the Czech and Polish Sudetes (Jizerske hory, Krkonose Mountains and Orlice-Sneznik Complex). Int J Earth Sci 90: 304–324

Kryza R, Zalasiewicz JA, Mazur S, Aleksandrowski P, Sergeev S, Presnyakov S (2007) Early Palaeozoic initial-rift volcanism in the central European variscides (the Kaczawa Mountains, Sudetes, SW Poland): evidence from SIMS dating of zircons. J Geol Soc London 164: 1207–1215

Kryza R, Zalasiewicz J, Rodionov N (2008) Enigmatic sedimentary-volcanic successions in the central European I Variscides: a Cambrian/Early ordovician age for the Wojcieszow Limestone (Kaczawa Mountains, SW Poland) indicated by SHRIMP dating of volcanic zircons. Geol J 43: 415–430

Kuster D, Liegeois JP, Matukov D, Sergeev S, Lucassen F (2008) Zircon geochronology and Sr, Nd, Pb isotope geochemistry of granitoids from Bayuda Desert and Sabaloka (Sudan): Evidence for a Bayudian event (920-900 Ma) preceding the Pan-African orogenic cycle (860-590 Ma) at the eastern boundary of the Saharan Metacraton. Precambrian Res 164: 16–39

Lange U, Brocker M, Armstrong R, Zelazniewicz A, Trapp E, Mezger K (2005) The orthogneisses of the Orlica-Snieznik complex (West Sudetes, Poland): geochemical characteristics, the importance of pre-Variscan migmatization and constraints on the cooling history. J Geol Soc London 162: 973–984

Linnemann U, Romer RL (2002) The Cadomian Orogeny in Saxo-Thuringia, Germany: geochemical and Nd-Sr-Pb isotopic characterization of marginal basins with constraints to geotectonic setting and provenance. Tectonophysics 352: 33–64

Linnemann U, Mcnaughton N J, Romer RL, Gehmlich M, Drost K, Tonk C (2004) West African provenance for Saxo-Thuringia (Bohemian Massif): Did Armorica ever leave pre-Pangean Gondwana? - U-Pb-SHRIMP zircon evidence and the Nd-isotopic record. International Journal of Earth Sciences 93: 683–705

Linnemann U, Gerdes A, Drost K, Buschmann B (2007) The continuum between Cadomian Orogenesis and opening of the Rheic Ocean: Constraints from LA-ICP-MS U-Pb zircon dating and analysis of plate-tectonic setting (Saxo-Thuringian Zone, NE Bohemian massif, Germany).

In: Linnemann U, Nance D, Kraft P, Zulauf G (eds) The Evolution of the Rheic Ocean: From Avalonian-Cadomian Active Margin to Alleghenian-Variscan Collision. Geological Society of America, Boulder, Colorado, Special Paper 423: 61–96

Martínez Catalán JR, Arenas R, Díaz García F, Abati J (1997) Variscan accretionary complex of northwest Iberia: Terrane correlation and succession of tectonothermal events. Geology 25: 1103–1106

Mazur S, Kroner A, Szczepanski J, Turniak K, Hanzl P, Melichar R, Rodionov NV, Paderin I, Sergeev SA (2010) Single zircon U-Pb ages and geochemistry of granitoid gneisses from SW Poland: evidence for an Avalonian affinity of the Brunian microcontinent. Geol Mag 147: 508–526

Melleton J, Cocherie A, Faure M, Rossi P (2010) Precambrian protoliths and Early Paleozoic magmatism in the French Massif Central: U-Pb data and the North Gondwana connection in the west European Variscan belt. Gondwana Res 17:13–25

Mingram B, Kröner A, Hegner E, Krentz O (2004) Zircon ages, geochemistry, and Nd isotopic systematics of pre-Variscan orthogneisses from the Erzgebirge, Saxony (Germany), and geodynamic interpretation. Int J Earth Sci 93: 706–727

Montero P, Bea F (1998) Accurate determination of $^{87}Rb/^{86}Sr$ and $^{143}Sm/^{144}Nd$ ratios by inductively-coupled-plasma mass spectrometry in isotope geoscience: an alternative to isotope dilution analysis. Anal Chim Acta 358: 227–233

Montero P, Bea F, González-Lodeiro F, Talavera C, Whitehouse M (2007) Zircon crystallization age and protolith history of the metavolcanic rocks and metagranites of the Ollo de Sapo Domain in central Spain. Implications for the Neoproterozoic to Early-Paleozoic evolution of Iberia. Geol Mag 144: 963–976

Montero MP, Talavera C, Bea F, González Lodeiro F, Whitehouse M (2009) Zircon Geochronology of the Ollo de Sapo Formation and the age of the Cambro-Ordovician rifting in Iberia. The Journal of Geology 117: 174–191

Murphy JB, Gutierrez Alonso G, Fernández Suárez J, Braid JA (2008) Probing crustal and mantle lithosphere origin through Ordovician volcanic rocks along the Iberian passive margin of Gondwana. Tectonophysics 461: 166–180

Nance RD, Gutierrez-Marco G, Keppie JD, Linnemann U, Murphy JB, Quesada C, Strachan RA, Woodcock NH (2010) Evolution of the Rheic Ocean. Gondwana Res 17: 194–222

Neiva AMR, Williams IS, Ramos JMF, Gomes MEP, Silva MMVG, Antunes IMHR (2009) Geochemical and isotopic constraints on the petrogenesis of Early Ordovician granodiorite and Variscan two-mica granites from the Gouveia area, central Portugal. Lithos 111: 186–202

Oberc-Dziedzic T, Kryza R, Mochnacka K, Larionov A (2010) Ordovician passive continental margin magmatism in the Central-European Variscides: U-Pb zircon data from the SE part of the Karkonosze-Izera Massif, Sudetes, SW Poland. Int J Earth Sci 99: 27–46

Oggiano G, Gaggero L, Funedda A, Buzzi L, Tiepolo M (2010) Multiple early Paleozoic volcanic events at the northern Gondwana margin: U-Pb age evidence from the Southern Variscan branch (Sardinia, Italy). Gondwana Res 17: 44–58

Pearce NJG, Perkins WT, Westgate JA, Gorton MP, Jackson SE, Neal CR, Chenery SP (1997) A Compilation of New and Published Major and Trace Element Data for NIST SRM 610 and NIST SRM 612 Glass Reference Materials. Geostandards Newsletters 21, 115–144

Pérez-Estaún A, Bea F (2004). Macizo Ibérico. In: Vera JA (ed.) Geología de España, 1st edn. Madrid, pp 19–230

Pin C, Waldhausrova J (2007). Sm-Nd isotope and trace element study of Late Proterozoic metabasalts (spillites) from the Central Barradian domain (Bohemian Massif, Czech Republic). Geological Society of America, Special Papers 423: 231–247

Pouclet A, Ouazzani H, Fekkak A (2008). The Cambrian volcano-sedimentary formations of the westernmost High Atlas (Morocco): their place in the geodynamic evolution of the West African Palaeo-Gondwana northern margin. In: Ennih N, Liégeois JP (eds.) The Boundaries of West African Craton. London, pp 303–327

Ries AC, Shackleton RM (1971) Catazonal complexes of North-West Spain and North Portugal, renmants of a Hercynian thrust plate. Nature Physical Sciences 234: 65–68

Siebel W, Trzebski R, Stettner G, Hecht L, Casten U, Hohndorf A, Muller P (1997) Granitoid magmatism of the NW Bohemian massif revealed: Gravity data, composition, age relations and phase concept. Geol Rundsch 86: Suppl.: S45–S63

Sola AR, Pereira MF, Ribeiro ML, Neiva AMR, Williams IS, Montero, P, Bea F, Zinger T, (2006) The Urra Formation: Age and Precambrian inherited record. VII Congresso Nacional de Geologia de Portugal

Sola AR (2007). Relaçoes petrogeoquímicas dos Maciços Graníticos do NE Alentejano. Ph.D. thesis, Universidade de Coimbra, Lisboa .

Sola AR, Pereira MF, Williams IS, Ribeiro ML, Neiva AMR, Montero P, Bea F, Zinger T (2008) New insights from U-Pb zircon dating of Early Ordovician magmatism on the northern Gondwana margin: The Urra Formation (SW Iberian Massif, Portugal). Tectonophysics 461: 114–129

Stacey JS, Kramers JD (1975) Approximation of terrestrial lead isotope evolution by a two-stage model. Earth Planet Sc Lett 26: 207–221

Steiger RH, Jäger E (1977) Subcommision on Geochronology. Convention on the use of decay constants in geo- and cosmochronology. Earth Planet Sc Lett 36: 359–362

Talavera C, Montero P, Bea F (2008) Precise single-zircon Pb-Pb dating reveals that Aljucén (Mérida) is the oldest plutonic body of the Central Iberian Zone. Geo-Temas 10: 249–252

Teipel U, Eichhorn R, Loth G, Rohrmuller J, Holl R, Kennedy A (2004) U-Pb SHRIMP and Nd isotopic data from the western Bohemian Massif (Bayerischer Wald, Germany): Implications for Upper Vendian and Lower Ordovician magmatism. Int J Earth Sci 93: 782–801

Tichomirowa M, Berger HJ, Koch EA, Belyatski BV, Gotze J, Kempe U, Nasdala L, Schaltegger U (2001) Zircon ages of high-grade gneisses in the Eastern Erzgebirge (Central European Variscides) - constraints on origin of the rocks and Precambrian to Ordovician magmatic events in the Variscan foldbelt. Lithos 56: 303–332

Turniak K, Mazur S, Wysoczanski R (2000) SHRIMP zircon geochronology and geochemistry of the Orlica-Snieznik gneisses (Variscan belt of Central Europe) and their tectonic implications. Geodin Acta 13: 293–312

Villaseca, C., Belousova, E., Orejana, D., Castiñeiras, P., Pérez-Soba, C., 2011. Presence of

Palaeoproterozoic and Archean components in the granulite-facies rocks of central Iberia: The Hf isotopic evidence. Precambrian Res 187: 143–154

Walsh GJ, Aleinikoff JN, Benziane F, Yazidi A, Armstrong TR (2002) U-Pb zircon geochronology of the Paleoproterozoic Tagragra de Tata inlier and its Neoproterozoic cover, western Anti-Atlas, Morocco. Precambrian Res 117: 1–20

Whitehouse MJ, Kamber BS, Moorbath S (1999) Age significance of U-Th-Pb zircon data from early Archaean rocks of west Greenland - a reassessment based on combined ion-microprobe and imaging studies. Chem Geol 160, 201–224

Whitehouse MJ, Kamber BS (2005) Assigning Dates to Thin Gneissic Veins in High-Grade Metamorphic Terranes: A Cautionary Tale from Akilia, Southwest Greenland. J Petrol 46, 291–318.

Wiedenbeck M, Allé P, Corfu F, Griffin WL, Meier M, Oberli F, von Quadt A, Roddick JC, Spiegel W (1995) Three natural zircon standards for U-Th-Pb Lu-Hf trace element and REE analysis. Geostandards Newsletter 19: 1–23

Figure captions

Fig. 1 Outcrops of Cambro-Ordovician igneous rocks in Central Iberian and Galicia Tras-os-Montes Zones. Capital letters mean: CZ, Cantabric Zone; WALZ, Western Asturian Leonian Zone; CIZ, Central Iberian Zone; OSD, Ollo de Sapo Domain; SGCD, Schist-Graywacke Complex Domain; GTOMZ, Galicia Tras-os-Montes Zone; SD, Schistose Domain, AC, Allochthonous Complexes; BCSZ, Badajoz-Córdoba Shear Zone; OMZ, Ossa Morena Zone; SPZ, South Portuguese Zone

Fig. 2 Geological Scheme of alignment of the Cambro-Ordovician igneous rocks from northern part of the Schist-Graywacke Complex Domain. The geological scheme represents a section of the geological map of Spain (Alvaro et al. 1994). All the Cambro-Ordovician igneous bodies have been analyzed for U-Pb zircon geochronology except Santa Maria de la Alameda, Navas del Marqués and Prádena del Rincón

Fig. 3 Geological Scheme of alignment of the Cambro-Ordovician igneous rocks from Schistose Domain of Galicia Tras-os-Montes Zone. The geological scheme represents a section of the geological map of Spain (Alvaro et al. 1994). All the Cambro-Ordovician igneous bodies have been analyzed for U-Pb zircon geochronology except Sisargas

Fig. 4 U-Pb data plotted in Tera-Wasserburg (A) and Wetherill (B) concordias of: 1-Fermoselle; 2-Vitigudino; 3-Ledesma; 4-San Pelayo; 5-Castellanos; 6-Bercimuelle;. Crosses represent LA-ICPMS data and circles represent ion microprobe data

Fig. 5 U-Pb data plotted in Tera-Wasserburg (A) and Wetherill (B) concordias of: 1-La Cañada; 2-La Hoya; 3-La Estación I; 4-La Estación II; 5-Vegas de Matute (melanocratic); 6-Vegas de Matute (leucocratic). Crosses represent LA-ICPMS data and circles represent ion microprobe data

Fig. 6 U-Pb SIMS data plotted in Tera-Wasserburg (A) and Wetherill (B) concordias of: 1-La Morcuera; 2-Buitrago de Lozoya; 3-La Berzosa; 4-El Cardoso; 5-Riaza; 6-Polán

Fig. 7 U-Pb SIMS data plotted in Tera-Wasserburg (A) and Wetherill (B) concordias of Mohares

Fig. 8 U-Pb data plotted in Tera-Wasserburg (A) and Wetherill (B) concordias of: 1-Cherpa;

2-Noia; 3-Laxe; 4-Pontevedra; 5-Vilanova; 6-Bangueses. Crosses represent LA-ICPMS data and circles represent ion microprobe data

Fig. 9 U-Pb data plotted in Tera-Wasserburg (A) and Wetherill (B) concordias of: 1-Bande; 2-Rial de Sabucedo; 3- San Mamede. Crosses represent LA-ICPMS data and circles represent ion microprobe data

Fig. 10 Cathodoluminescence images and ages of selected zircons of Castilian and Galician gneisses

Fig. 11 Age distribution pattern found in zircons of Castilian and Galician gneisses. Built from U-Pb SIMS and LA-ICPMS data of these rocks

Fig. 12 Distribution of the U-Pb zircon ages for: 1) metagranites and metavolcanic rocks from Ollo de Sapo Domain; 2) Urra Formation and Portalegre and Carrascal granitoids; and 3) Castilian and Galician gneisses. Built from U-Pb SIMS and LA-ICPMS data of these rocks

Fig. 13 $(\epsilon_{Nd})_{485Ma}$ versus $(^{87}Sr/^{86}Sr)_{485Ma}$. Circles represent isotopic data of Cambro-Ordovician igneous rocks from the Ollo de Sapo Domain, crosses represent isotopic data from Castillian and Galician gneisses, triangles represent isotopic data from Urra Formation and Portalegre and Carrascal granitoids and squares represent isotopic data from Oledo and Gouveia granitoids

Fig. 14 Distribution of the U-Pb zircon ages for the Cambro-Ordovician metagranites and metavolcanic rocks from European Variscan Belt. Built from U-Pb SIMS and LA-ICPMS data of Bertrand et al. 2000; Turniak et al. 2000; Deloule et al. 2002; Guillot et al. 2002; Drost et al. 2004; Friedl et al. 2004; Linnemann et al 2004; Mingram et al. 2004; Teipel et al. 2004; Helbing and Tiepolo 2005; Giacomini et al. 2006; Alexandre 2007; Kryza et al. 2007; Linnemann et al 2007; Castiñeiras et al. 2008; Kryza et al. 2008; Mazur et al. 2010; Melleton et al. 2010; Oberc-Dziedzic et al. 2010; Oggiano et al. 2010

Fig 15 Distribution of the U-Pb zircon ages for Cambro-Ordovician igneous rocks from European Variscan Belt (including Central Iberian Zone) and Panafrican igneous rocks from Saharan Metacraton and West African Craton

Fig. 16 $(\epsilon_{Nd})_{485Ma}$ versus $(^{87}Sr/^{86}Sr)_{485Ma}$. Circles and crosses represent isotopic data of Cambro-Ordovician igneous rocks from Central Iberian Zone and other outcrops of European Variscan Belt and triangles, Xs and squares represent isotopic data of Panafrican igneous rocks from European Variscan Belt, Saharan Metacraton and West African Craton. Isotopic data of Kroner et al. 1994; Kroner et al. 1995; Siebel et al. 1997; Kroner and Hegner 1998; Kroner et al. 2001; Tichomirowa et al. 2001; Chen et al. 2002; Linnemann and Romer 2002; Bandrés et al. 2004; Mingram et al. 2004; Teipel et al. 2004; Lange et al. 2005; Montero et al. 2007; Pin and Waldhausrova 2007; Sola 2007; Hasalova et al. 2008; Sola et al. 2008; Antunes et al. 2009; Montero et al. 2009; Neiva et al. 2009

Fig. 17 Distribution of Nd model ages (T_{DM}) for Cambro-Ordovician igneous rocks from the European Variscan Belt and Panafrican igneous rocks from Saharan Metacraton and West African Craton

Table captions

Table 1 Summary of the crystallization ages of the Castilian and Galician gneisses. Note that Navas del Marques, Santa María de la Alameda, Prádena del Rincón and Sisargas have not been analyzed for U-Pb zircon geochronology in this paper.

Table 2 Sr-Nd isotope composition of selected Castilian and Galician gneisses

Table 3 U-Pb ion microprobe and laser ablation results of Castilian gneisses. Subscript "m" for isotope ratios means measured. For grains with the same reference, the characters "c" and "b" mean core and rim, respectively.

Table 4 U-Pb ion microprobe and laser ablation results of Galician gneisses. Subscript "m" for isotope ratios means measured. For grains with the same reference, the characters "c" and "b" mean core and rim, respectively.

Figure1
Click here to download Figure: Fig1.pdf

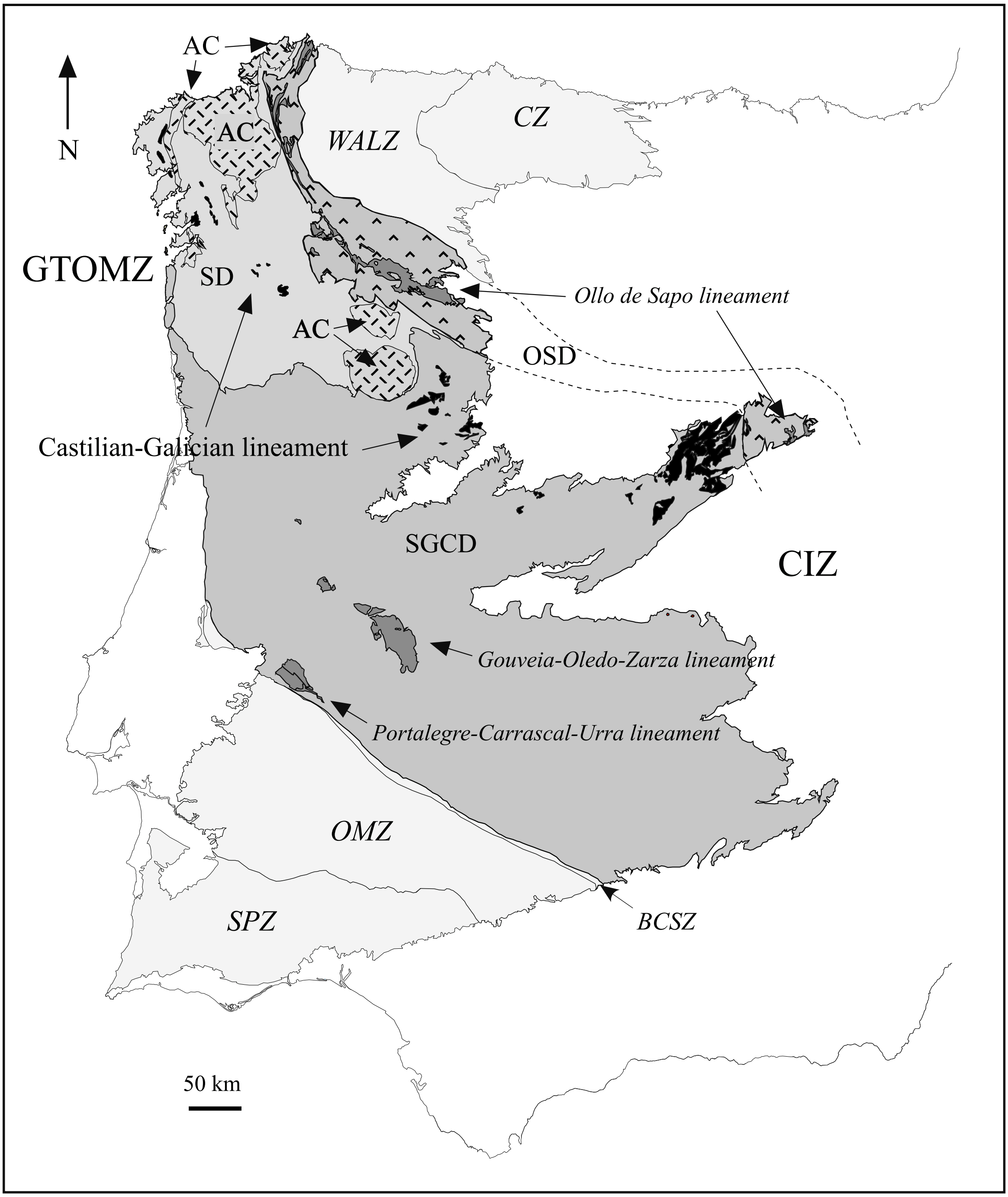

Figure2

Click here to download Figure: Fig2.pdf

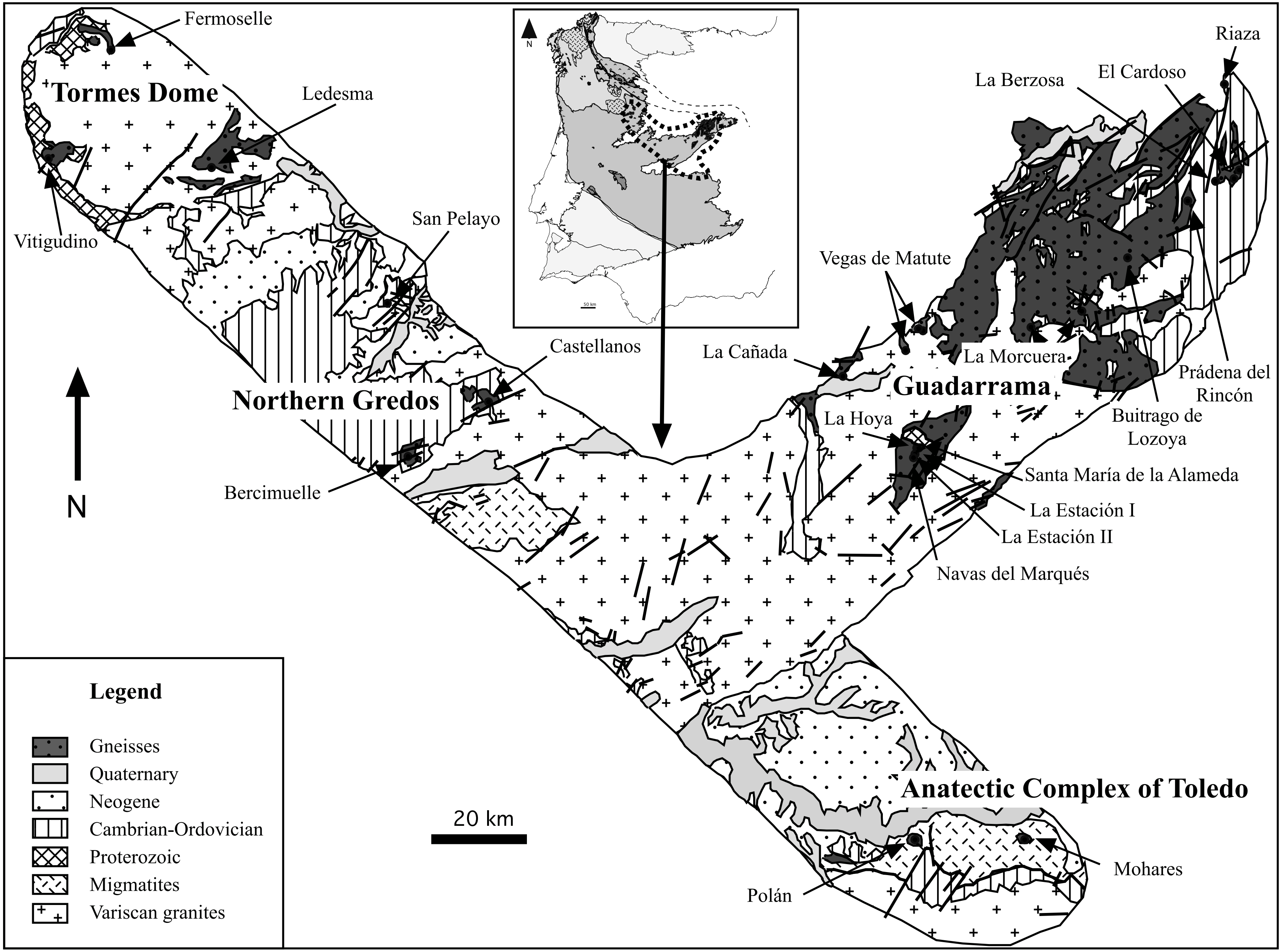

Figure3

Click here to download Figure: Fig3.pdf

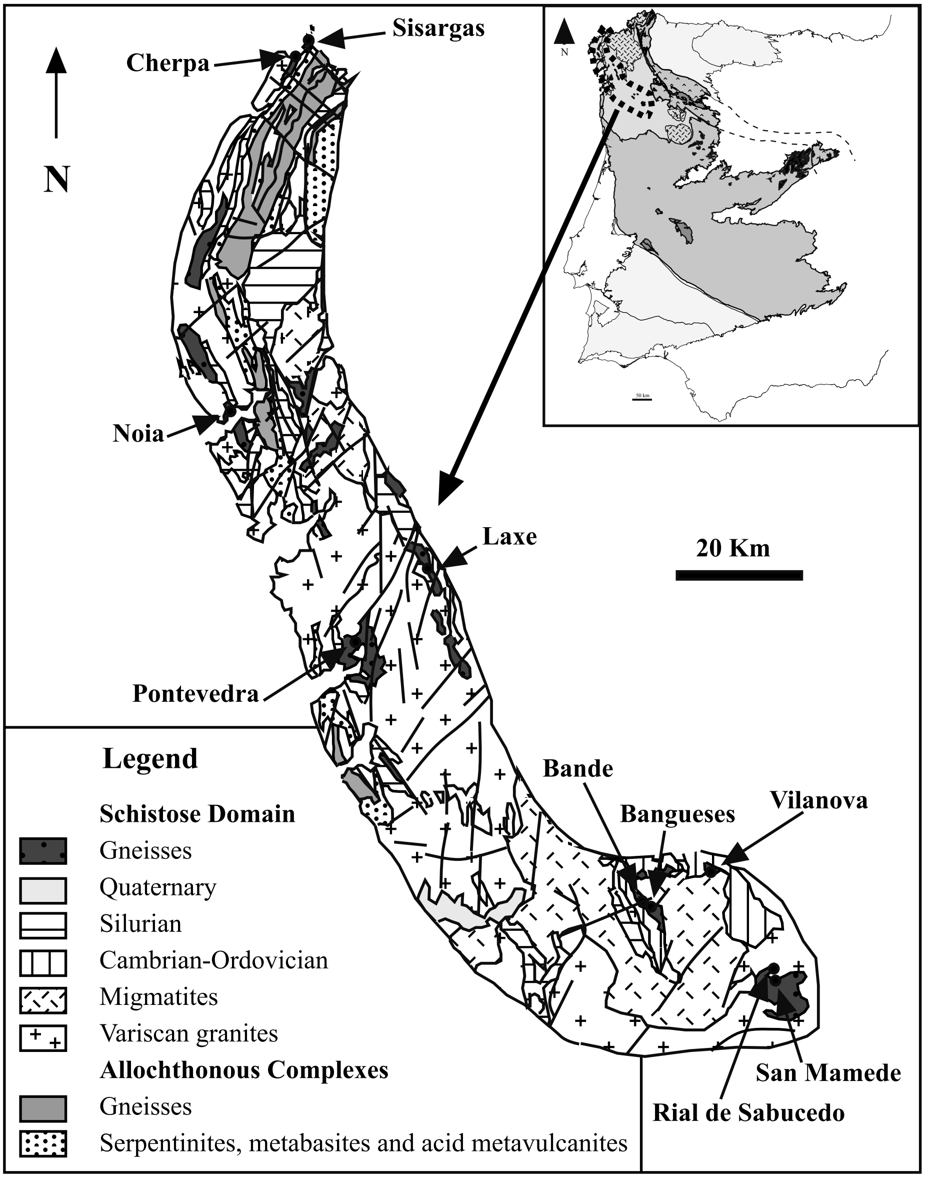

Figure4

Click here to download Figure: Fig4.pdf

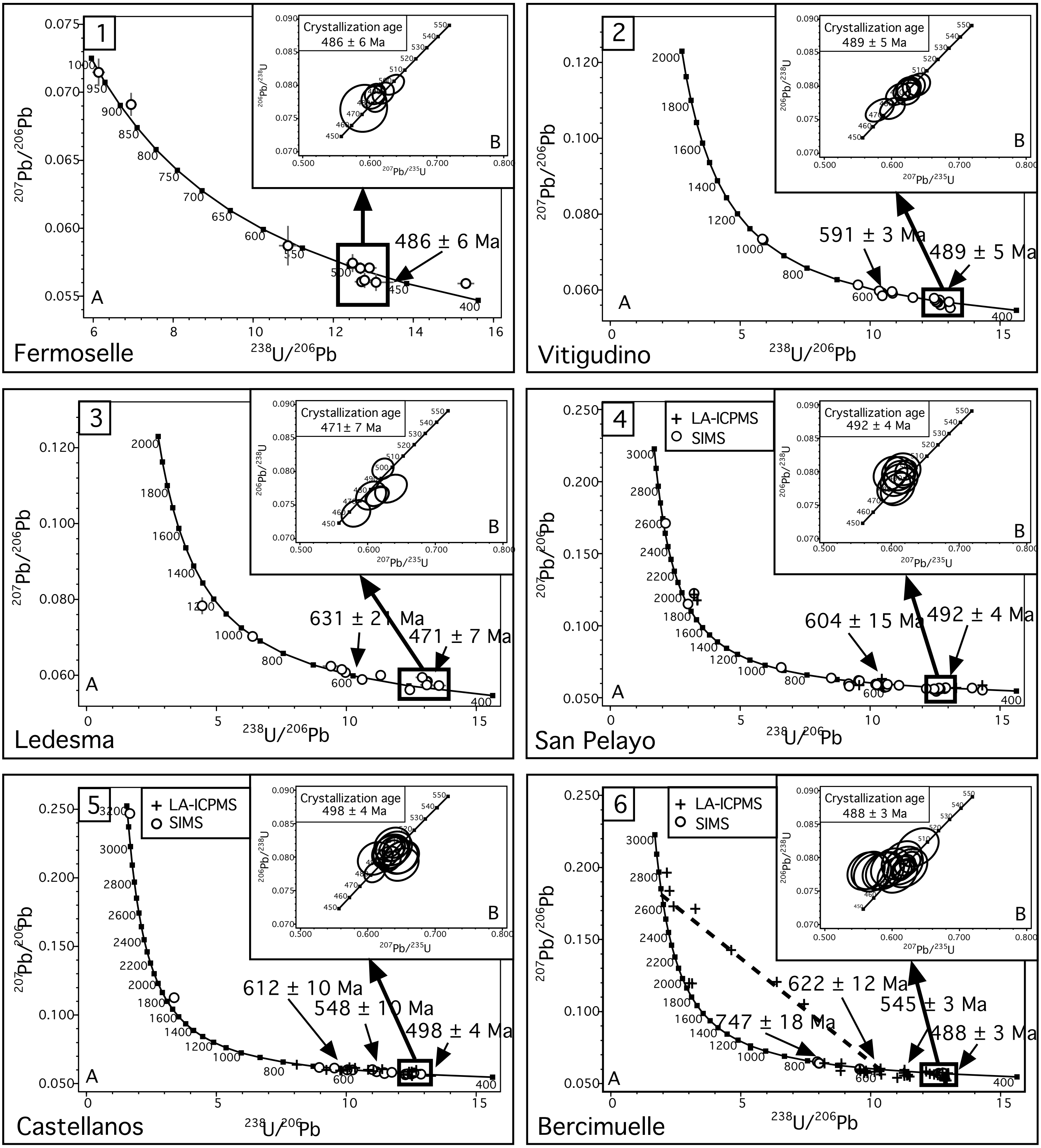

Figure5
Click here to download Figure: Fig5.pdf

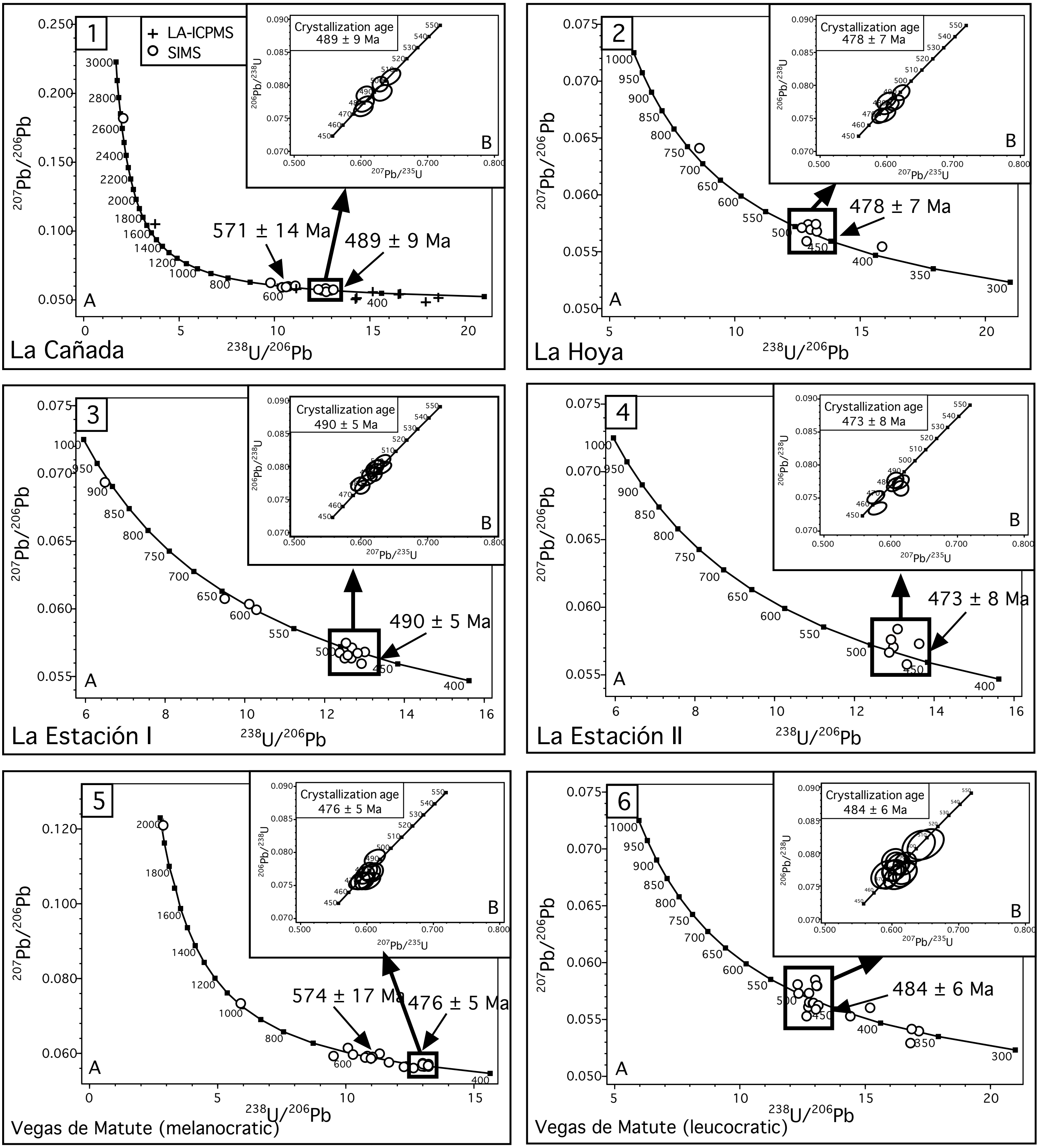

Figure6

Click here to download Figure: Fig6.pdf

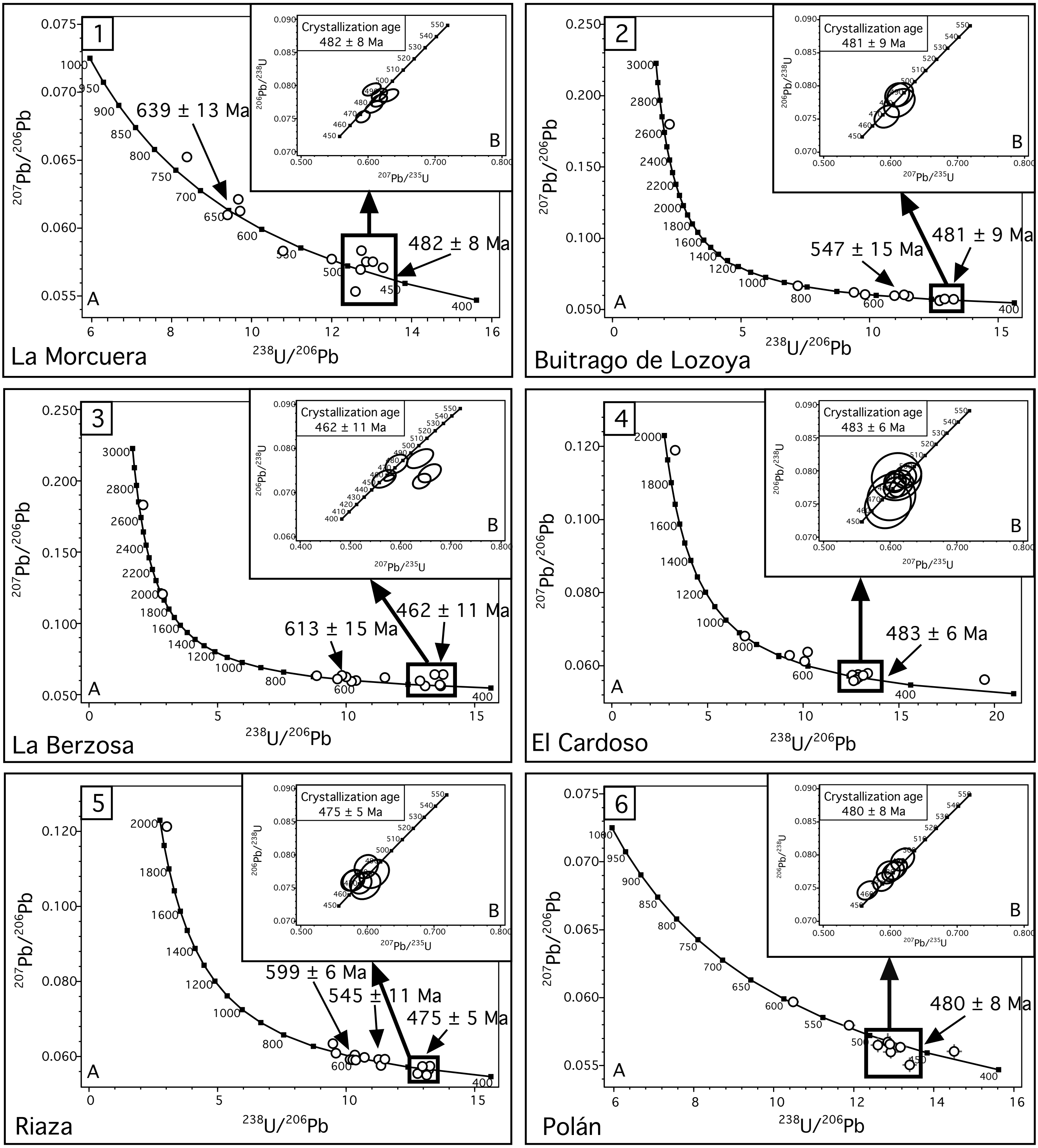

Figure7
Click here to download Figure: Fig7.pdf

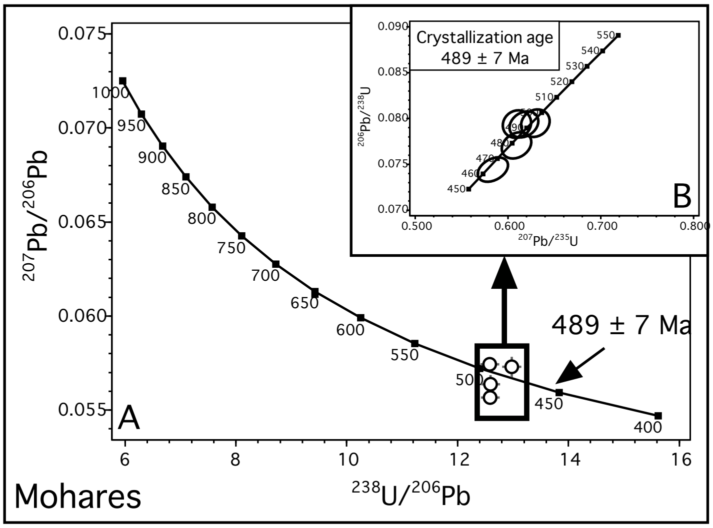

Figure8

Click here to download Figure: Fig8.pdf

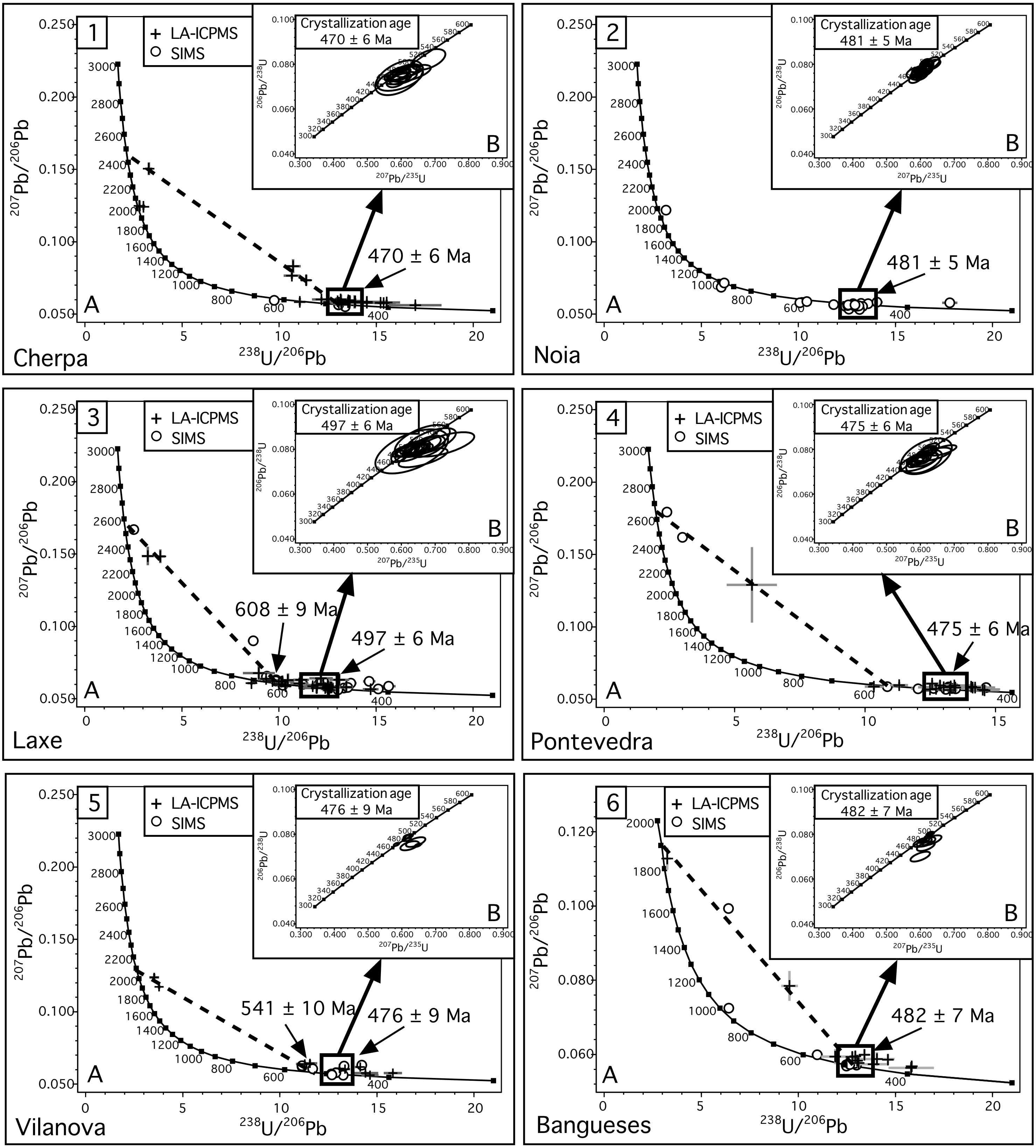

Figure9

Click here to download Figure: Fig9.pdf

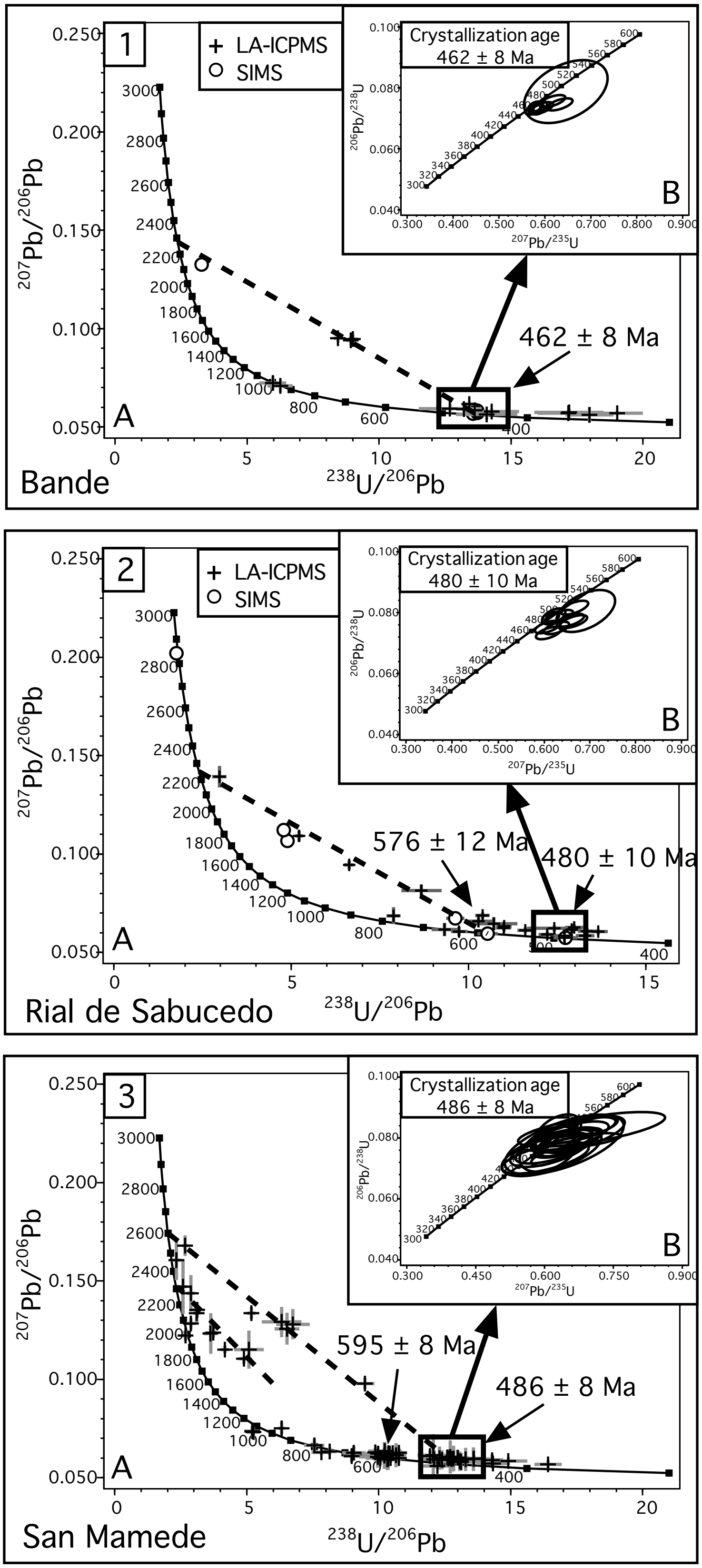

Figure10
Click here to download Figure: Fig10.pdf

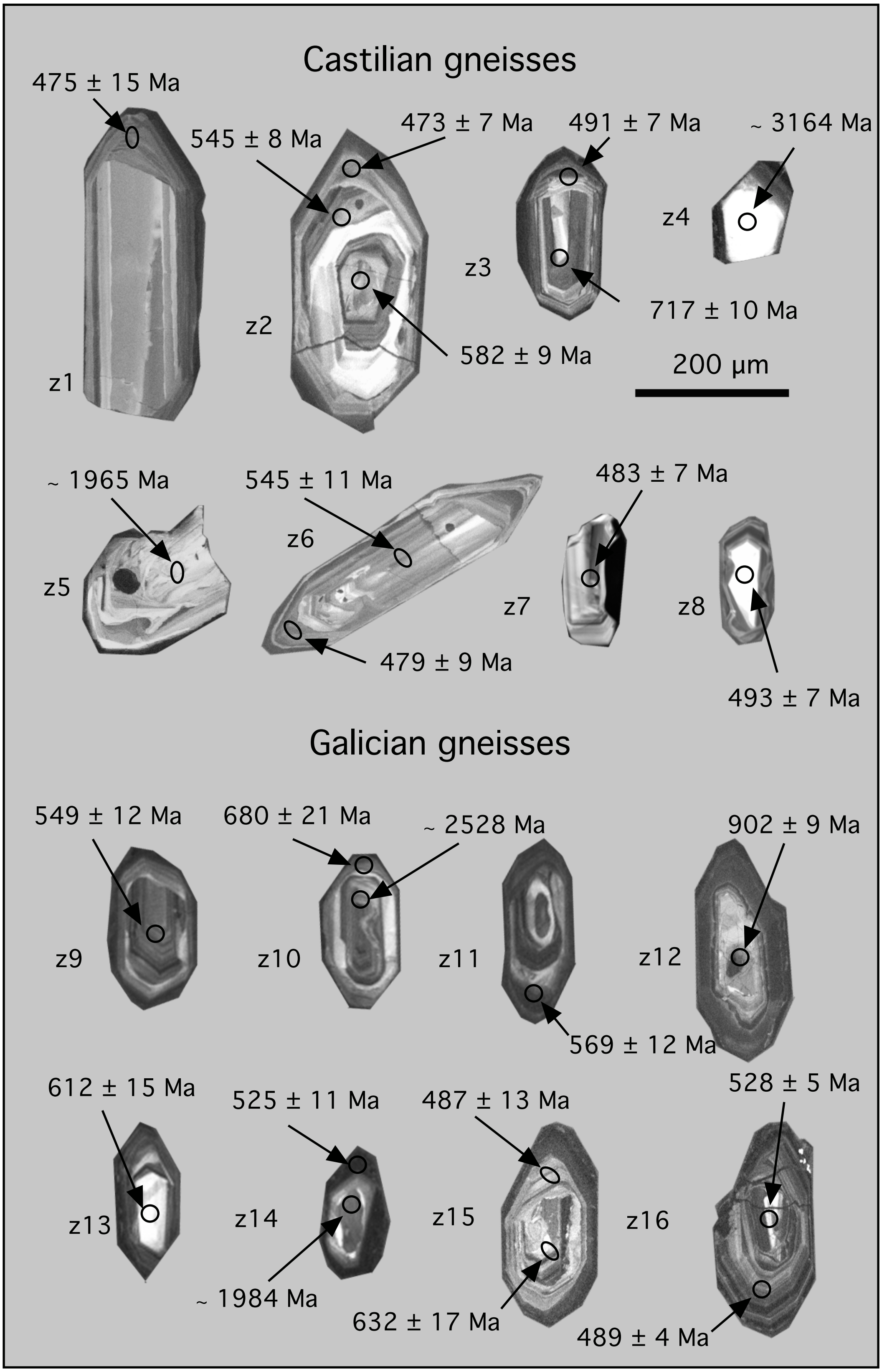

Figure11
Click here to download Figure: Fig11.pdf

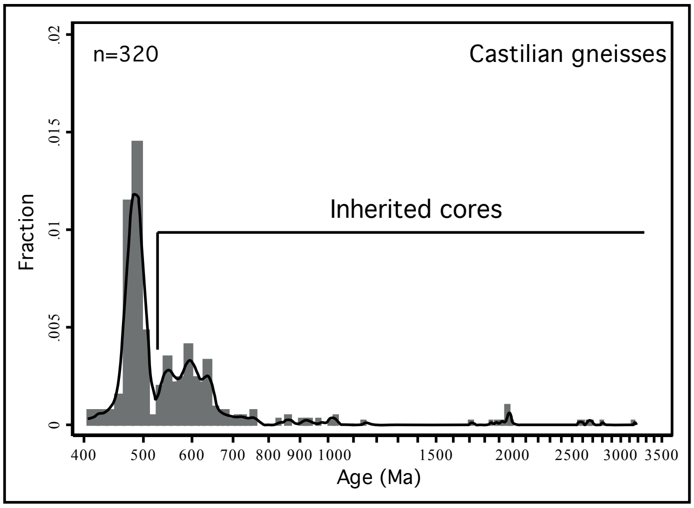

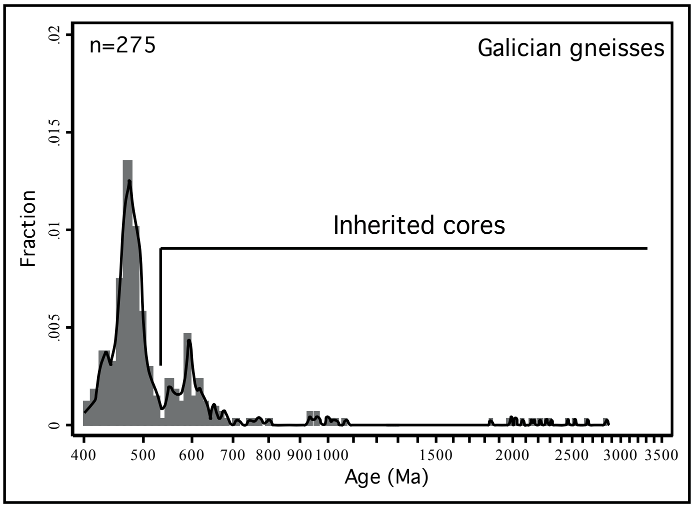

Figure12
Click here to download Figure: Fig12.pdf

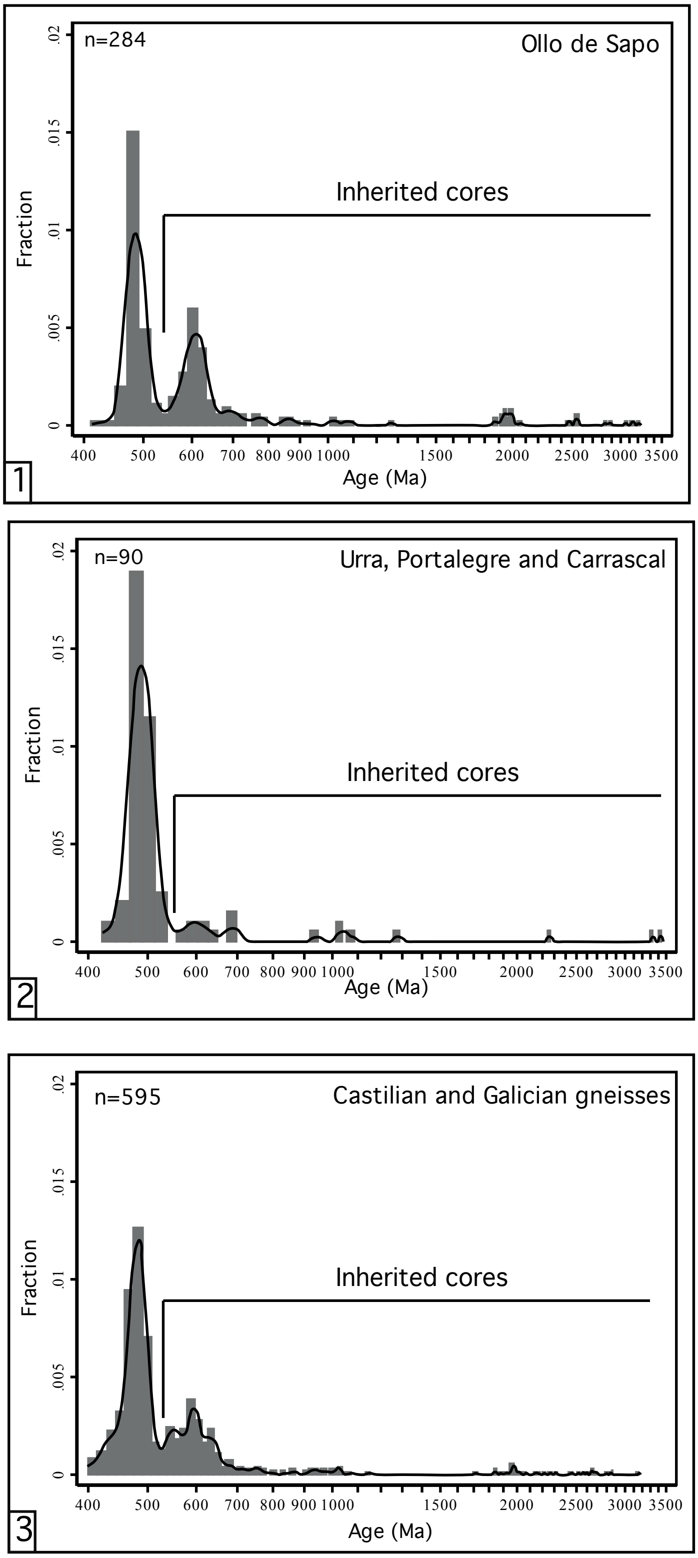

Figure13

Click here to download Figure: Fig13.pdf

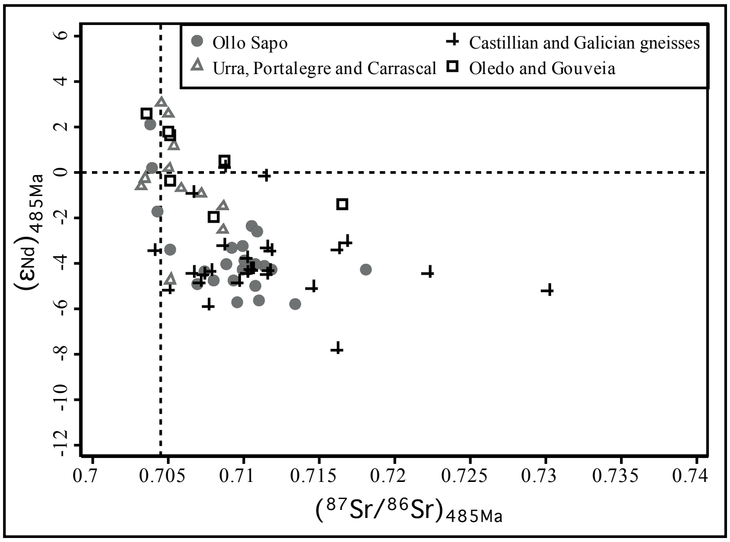

Figure14

Click here to download Figure: Fig14.pdf

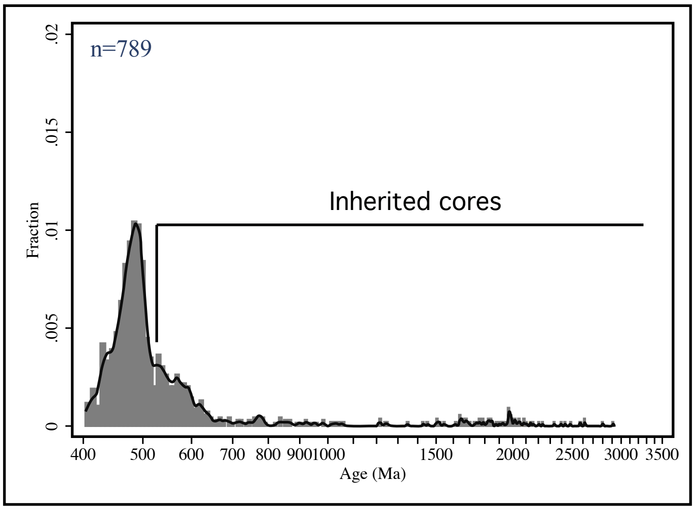

Figure15
Click here to download Figure: Fig15.pdf

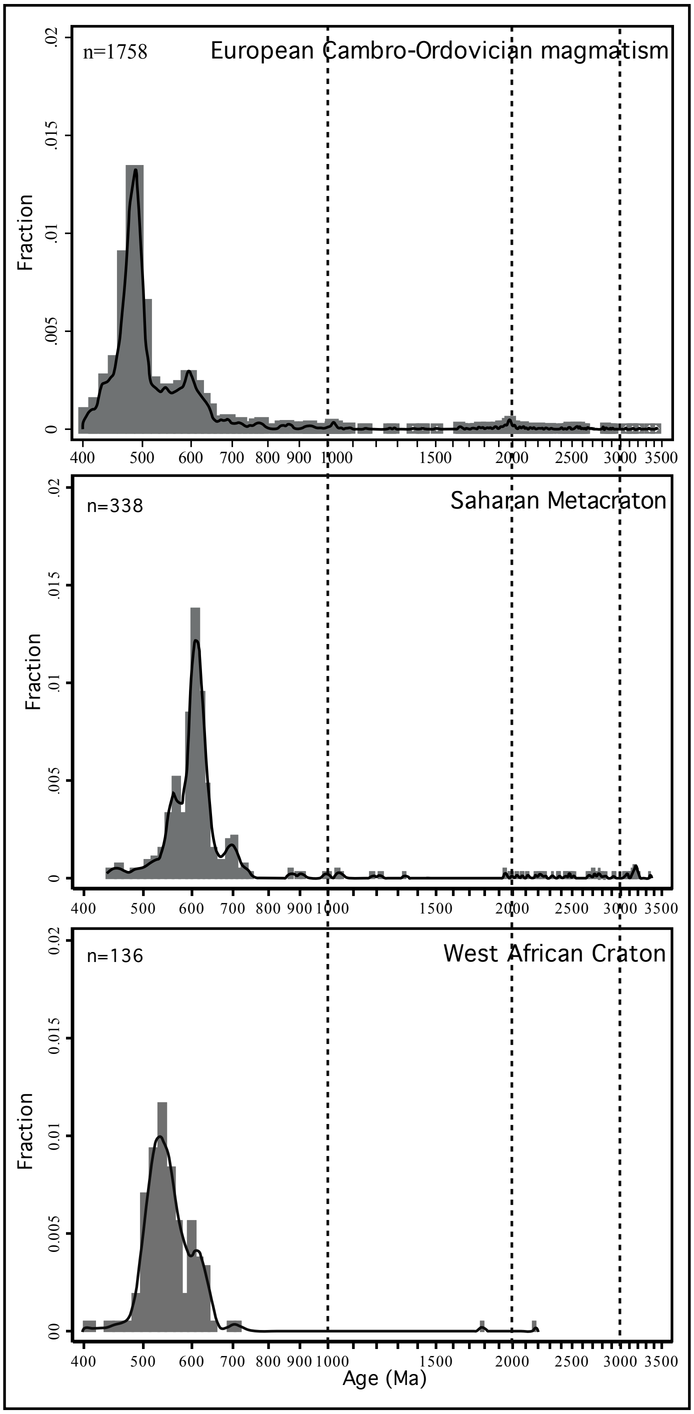

Figure16

Click here to download Figure: Fig16.pdf

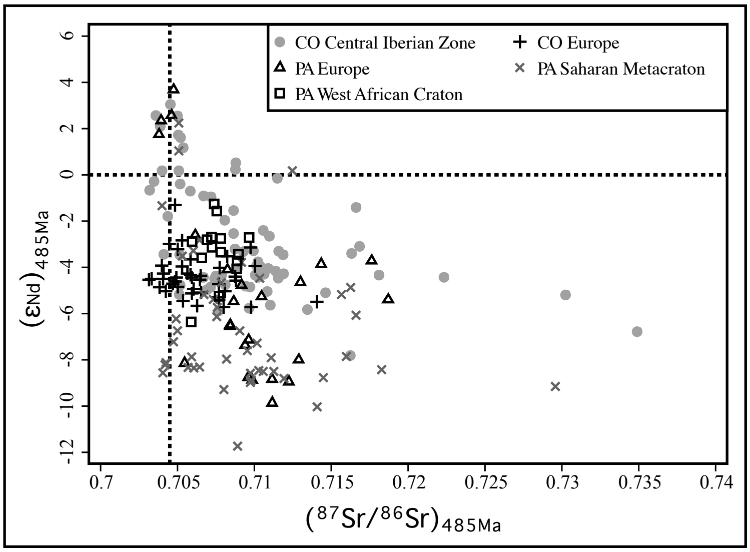

Figure17
Click here to download Figure: Fig17.pdf

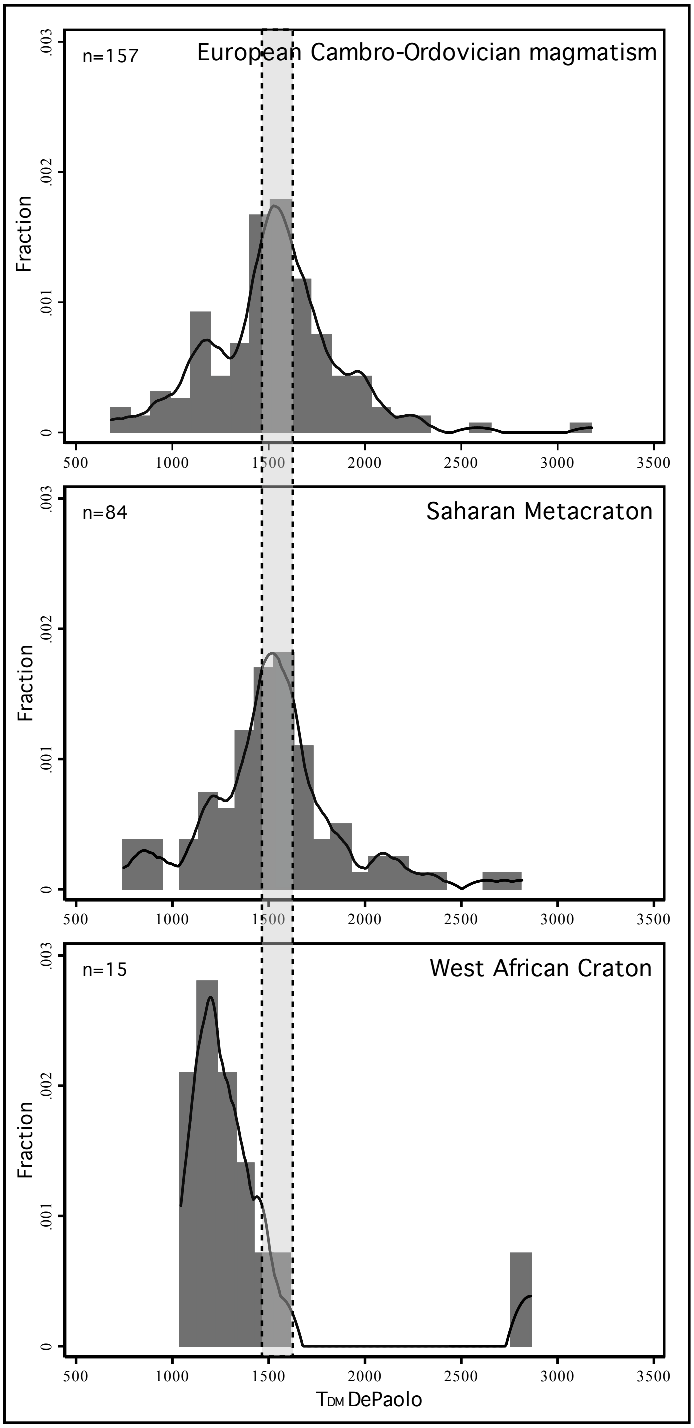

Geological unit	Crystallization age	Coordinates	
Castillian gneisses			
The Tormes Dome			
Fermoselle metagranite	486 ± 6 Ma	728410	4569184
Vitigudino metagranite	489 ± 5 Ma	713570	4550750
Ledesma metagranite	471 ± 7 Ma	749762	4554165
Northern Gredos			
San Pelayo metagranite	492 ± 4 Ma	282704	4519025
Castellanos metagranite	498 ± 4 Ma	304519	4502133
Bercimuelle metagranite	488 ± 3 Ma	287519	4489185
Guadarrama			
La Cañada metagranite	489 ± 9 Ma	377827	4506869
La Hoya metagranite	478 ± 7 Ma	393596	4492690
La Estación metagranite	490 ± 5 Ma (La Estación I) 473 ± 8 Ma (La Estación II)	392901 392958	4491933 4492249
Vegas de Mature metagranite	476 ± 5 Ma (melanocratic) 484 ± 6 Ma (leucocratic)	394508 391096	4516599 4515720
La Morcuera metagranite	482 ± 8 Ma	429941	4519575
Buitrago de Lozoya metagranite	481 ± 9 Ma	439556	4532323
La Berzosa metavolcanic rocks	462 ± 11 Ma	457358	4545281
El Cardoso metavolcanic rocks	483 ± 6 Ma	461621	4547336
Riaza metavolcanic rocks	475 ± 5 Ma	461360	4568843
Anatectic Complex of Toledo			
Polán metagranite	480 ± 8 Ma	401453	4412943
Mohares metagranite	489 ± 7 Ma	424126	4409789
Galician gneisses			
Cherpa metagranite	470 ± 6 Ma	511182	4796304
Noia metagranite	481 ± 5 Ma	503203	4736750
Laxe metagranite	497 ± 6 Ma	537117	4715775
Pontevedra metagranite	475 ± 6 Ma	525242	4700895
Vilanova metagranite	476 ± 9 Ma	586459	4669168
Bangueses metagranite	482 ± 7 Ma	578705	4661739
Bande metagranite	462 ± 8 Ma	579229	4660190
Rial de Sabucedo metagranite	480 ± 10 Ma	599056	4653924
San Mamede metagranite	486 ± 8 Ma	599326	4653207

Table2

Sample	Geological unit	Rb	Sr	($^{87}Sr/^{86}Sr$)	Sm	Nd	($^{143}Nd/^{144}Nd$)
Castilian gneisses							
CTS-49	Vitigudino metagranite	229	36	0.846156	4.1	17.8	0.512278
CTS-50	Fermoselle metagranite	255	61	0.791986	4.2	18.3	0.512152
GNB-2	Bercimuelle metagranite	242	78	0.770138	4.9	22.3	0.512208
GNB-3	Bercimuelle metagranite	229	87	0.764712	5.9	26.7	0.512264
GNB-5	Castellanos metagranite	146	80	0.745292	4.8	21.4	0.512276
GNB-6	Castellanos metagranite	188	115	0.763038	6.7	32.8	0.512138
CT-102	Navas del Marqués metagranite	213	78	0.761197	4.0	18.2	0.512209
CT-104	Santa María de la Alameda metagranite	227	81	0.760297	10.0	49.5	0.512224
CT-105	La Hoya metagranite	165	137	0.740912	6.9	33.7	0.512246
CT-108	La Estación I metagranite	189	91	0.75353	3.5	15.3	0.512231
CT-110	Riaza metavolcanic rocks	230	72	0.774627	4.0	18.0	0.512212
CT-112	El Cardoso metavolcanic rocks	154	232	0.723931	8.9	43.7	0.512185
CT-114	El Cardoso metavolcanic rocks	149	167	0.727581	7.4	35.5	0.512166
CT-116	Prádena del Rincón metagranite	275	55	0.818217	2.5	8.5	0.512169
CT-117	Buitrago de Lozoya metagranite	188	117	0.743759	6.1	28.9	0.512188
CT-118	La Morcuera metagranite	161	91	0.747097	10.3	46.4	0.512268
CT-122	Vegas de Matute (Melanocrátic) metagranite	130	187	0.724189	9.1	44.4	0.512212
CT-123	La Berzosa metavolcanic rocks	149	169	0.728115	6.8	34.2	0.512179
CT-124	La Berzosa metavolcanic rocks	241	71	0.782851	3.0	13.0	0.512191
Galician Gneisses							
CTG-14	Sisargas metagranite	260	63	0.794141	3.5	16.1	0.51242
CTG-15	Sisargas metagranite	276	54	0.811145	6.1	28.6	0.512436
CTG-16	Sisargas metagranite	327	60	0.817453	4.8	23.3	0.512359
CTG-20	Vilanova metagranite	295	27	0.943653	2.4	9.7	0.512266
CTG-22	Bande metagranite	308	34	0.889252	2.6	10.7	0.512222
CTG-46	Pontevedra metagranite	201	73	0.762198	7.5	32.7	0.512206
CTG-47	Pontevedra metagranite	207	86	0.756267	2.7	12.7	0.512202

$(^{87}Sr/^{86}Sr)_{485Ma}$	$(\quad)_{485}$	T_{DM}
0.71634	-3.41	1537
0.707704	-5.9	1801
0.707424	-4.5	1583
0.711875	-3.46	1492
0.708745	-3.22	1470
0.730262	-5.21	1517
0.706728	-4.44	1570
0.704132	-3.44	1353
0.716875	-3.1	1337
0.71177	-4.32	1625
0.710273	-4.44	1581
0.710652	-4.31	1443
0.709727	-4.86	1521
0.716246	-7.82	3610
0.711586	-4.49	1500
0.711588	-3.32	1467
0.710258	-3.78	1396
0.710496	-4.27	1414
0.714639	-5.11	1712
0.711505	-0.16	1141
0.708797	0.22	1099
0.706701	-0.92	1156
0.722342	-4.45	1886
0.705124	-5.18	1926
0.707182	-4.86	1696
0.707896	-4.35	1514